Registration No: 170170725

The University of Sheffield
Electrical and Electronic Engineering

Electronic Lock-in Amplifier for Low Cost Radiation Thermometry

Professor Chee Hing Tan

06/01/2020

1 Contents

2 Project Description and Aims

Accurate and repeatable measurement of temperature is a key issue across many industrial sectors, including the Pharmaceutical, Chemical and Steel Industries [1]. Factories require temperature measurements to regulate key production systems such as Furnaces, Wave or Reflow Soldering Machines and Curing Ovens. Currently, two primary methods of temperature measurement exist within industry: Contact Thermometers and Non-Contact Thermometers [2].

Contact Thermometers are the most widely used method within Industry, primarily due to their accuracy of measurement, value for money and ease of installation. Unfortunately, Contact Thermometers struggle to provide accurate measurements in high temperature environments due to interfering radiation from other objects around the detector [2]. This results in an average measurement of the contacted surface temperature and the wider environmental temperature [2].

Radiation Thermometers, part of the Non-Contact Thermometer family, measure the emitted infrared radiation from the target object in order to ascertain the surface temperature. This allows the Thermometer to be located outside the system or object being measured [2]. Consequently, environments too hot for a contact thermometer can be measured and maintenance becomes easier. Additionally, the issue of interfering radiation is resolved using optics to focus the Thermometers cone of measurement[1] onto a very small part of the object's surface.

Current industry standard Radiation Thermometers use PN or PIN Photodiodes as a detector. Photodiodes with a large Radiant Sensitive Area[2] are used to ensure accurate temperature measurements. This increases the spectral power hitting the detector, with the downside of increasing the cone of detection. An increased cone of detection results in the measurement becoming an average of an area of the objects surface rather than a desired single point measurement [2]. The maximum size of detectors is limited, resulting in small output signals from the photodiode (in the order of tens of *nA*). Thus, sensitive, low-noise circuitry is required to detect and measure these signals.

A common method of measuring low amplitude optical signals is to modulate the optical signal before detection using an Optical Chopper [3]. This modulated signal can then be measured using a Lock-in Amplifier (LIA, a form of phase sensitive detection [4]) by providing the frequency of modulation as a reference [4] [5]. **Figure 2.1** shows a standard setup for this method of measurement. Lock-in Amplifiers allow small signals to be extracted from a noise floor many times larger than the signal (upwards of 100dB of noise) [6]. The smaller the signal that can be detected, the smaller the dimensions of the photodiode can be. This allows for a cone of measurement close to a single point.

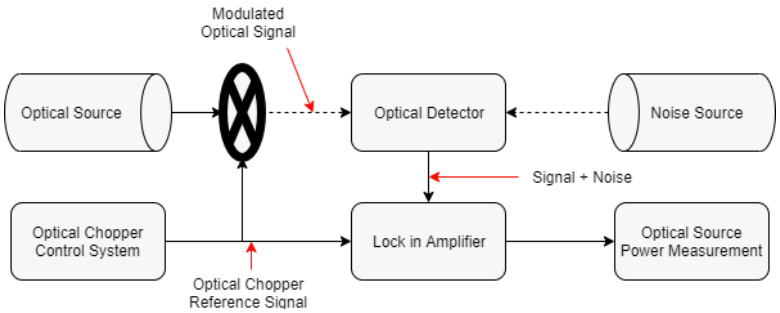

Figure 2.1: Standard Optical Chopper Measurement System Diagram

[1] The area of the measured surface the detector is receiving radiation from.

[2] The area of the Photodiode that is sensitive to incident photons.

Unfortunately, typical Lock-in Amplifiers cost upwards of £1000 [7]. Additionally, Optical Choppers are large mechanical components that require expensive calibration and regular maintenance. This places their reliability over time into question and makes them more complex to install in industrial environments.

This project aims to develop a low cost, fully Electronic Lock-in Amplifier for use in Radiation Thermometry applications. The Optical Chopper will be replaced with an electronic chopping circuit using two Photodiodes, as shown in **Figure 2.2**. One Photodiode acts as the detector for the Optical Source to be measured, whilst the other acts as a covered reference. The LIA circuit will build upon previous work completed by Tarick Osman [8].

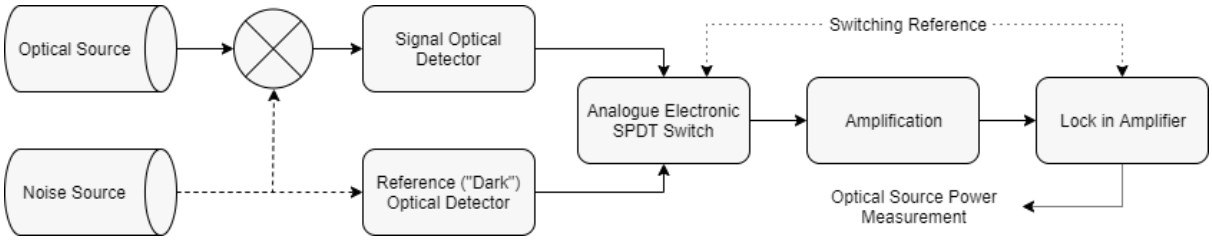

Figure 2.2: Electronic Chopper Measurement System Diagram

Additionally, this project aims to quantify the suitability of the Electronic Lock-in Amplifier for Radiation Thermometry. Existing and new designs will be compared against the Optical Chopper method to provide a comparison of small signal measurement performance.

3 Project Specification

No changes have been made to the project specification during the work performed since the Project Initialisation Document; consequently, the specification is the same as originally stated. To act as reference for this document and future sections of the project, the specification is presented again here.

The project has the following primary specifications[3]:

1. Explore the use of Electronic Lock-in Amplifiers for Radiation Thermometry by performing test measurements with existing hardware [8].
2. Improve the existing circuit [8] to detect below *nA*, aiming for *pA*.
    a. Construct a new Low Noise Transimpedance Amplifier with a gain to facilitate measurements in the *pA* range.
    b. Construct an Electronic Lock-in Amplifier with a filter appropriate for Radiation Thermometry.

Additionally, the project has the following stretch goals/specifications, should time allow for them:

- Investigate the use of Electronic Lock-in Amplifiers with Avalanche Photodiodes (APD) to evaluate the benefits and drawbacks of Avalanche Gain.
    a. Modify the constructed Lock-in Amplifier circuit for use with Avalanche Photodiodes.
    b. Compare and contrast the performance of the APD based system with PN/PIN Photodiodes.

[3] It is expected that objectives 1 and 2 will run in parallel.

4 Background Theory

This section outlines the background research conducted so far to facilitate the development and testing of the Electronic Lock-in Amplifier. Topics such as **Black Body Radiation** are covered to aide with Black Body source testing; whilst **Transimpedance Amplifiers** and **Voltage Amplifiers** are covered as part of the development of **Lock-in Amplifiers**.

4.1 Black Body Radiation

Black Body Radiation is the Electromagnetic Radiation emitted from objects above a uniform temperature of 0 Kelvin (*K*), usually from the Infrared and Visible sections of the spectrum between wavelengths of 0.5μm and 20μm [2]. A Black Body is an idealized object that is a perfect emitter of radiation; no such objects exist in the real world [2]. An example of an object close to a Black Body is the Sun, the star at the centre of our Solar System.

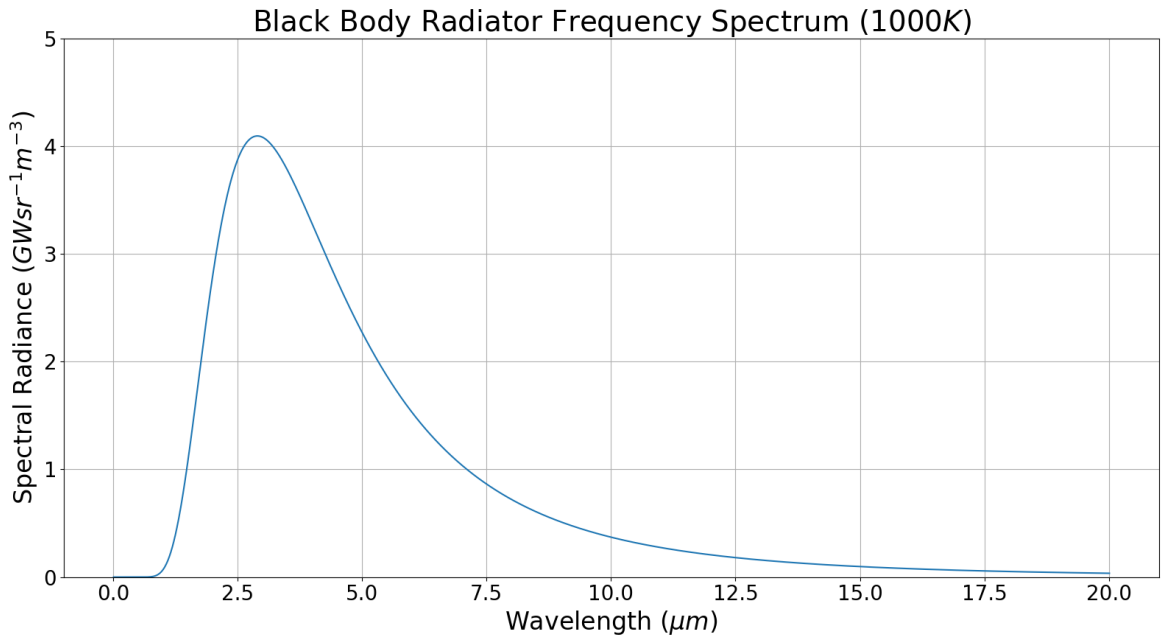

Figure 4.1: Example Frequency Spectrum of a Black Body

The frequency distribution of radiation emitted by the Black Body is proportional to its temperature in Kelvin [2]; it is not uniform. A typical distribution can be seen in **Figure 4.1**. The frequency spectrum of Black Bodies can be calculated by performing a sweep of **Equation 1**, Planck's Law [2].

$$L_b(\lambda, T) = \frac{c_1}{\lambda^5}\left[\exp\left(\frac{c_2}{\lambda T}\right) - 1\right]^{-1} \quad Wsr^{-1}m^{-3} \tag{1}$$

$$\mathrm{L} = \text{Spectral Radiance}$$

$$c_1 = 1.19104282 \times 10^{-16}\ \mathrm{Wm^{-2}}\ \text{(First Radiation Constant)}$$

$$c_2 = 0.014388\ \mathrm{K}\ \text{(Second Radiation Constant)}$$

Planck's Law gives the spectral radiance for a Black Body at a given temperature and wavelength. Performing a sweep of this calculation across relevant wavelengths gives the frequency spectrum of the Black Body.

The spectrum has a wavelength of peak intensity that is defined by the Black Body temperature; as the temperature of the Black Body increases the wavelength of peak intensity decreases. This explains why hot metals glow from bright white to dull red as their temperature decreases [2]. The wavelength of peak intensity can be calculated using **Equation 2**, Wein's Law [2].

$$\lambda_{max} = \frac{2898}{T} \mu m \tag{2}$$

Finally, the total spectral radiance of a Black Body can be calculated using **Equation 3**, the Stefan-Boltzmann Law [2]. The Stefan-Boltzmann law is obtained by integrating Planck's Law (**Equation 1**) over the entire Infrared spectrum.

$$M = \varepsilon \sigma T^4 \quad Wsr^{-1}m^{-2} \tag{3}$$

$$\mathrm{M} = \text{Total Spectral Radiance}, \varepsilon = \text{Emissivity}, \sigma = \text{Stefan-Boltzmann Constant}$$

Emissivity is a measure of how well an object radiates compared to a perfect Black Body radiator; it has a value between 0 and 1 [2]. Perfect Black Bodies have an emissivity of 1. All real-world objects have an emissivity less than 1; thus, they both reflect and absorb radiation [2].

4.2 Radiation Thermometry

Radiation Thermometry is the use of Electronic photo-detectors to measure the Black Body radiation from an object in order to determine surface temperature [2]. Having obtained a measurement of Total Spectral Radiance, the Stefan-Boltzmann Law (**Equation 3**) can be used to calculate the surface temperature of the object.

Unfortunately, measurements of the light emitted by a Black Body radiator are complicated by several factors. The measured value of optical power received from a source will be affected by the sources emissivity and reflectivity, as well as the absorption and scattering caused by the atmosphere between the source and detector [2].

As previously discussed in **Section 4.1**, emissivity is the measure of how well an object radiates. Unfortunately, emissivity introduces several problems for optical power measurement. Firstly, it is difficult to calculate the emissivity of many materials. Thus, we must rely on look up tables with measured values [2]. Secondly, emissivity is affected by the viewing angle of the detector relative to the surface being measured. This means the angle of installation for the detector must be calibrated during detector setup [2]. Finally, emissivity is not constant against radiation wavelength for most materials. Consequently, this variation must be compensated for when making a Total Spectral Radiance measurement [2]. Real world materials that have an approximately constant emissivity are known as Grey Bodys.

Reflectivity is the measure of how well radiation bounces off an object, instead of being absorbed by it. Reflectivity can make an object appear hotter, as interfering radiation from other sources reflects from the object into the detector [2].

Scattering is caused by particles between the radiation source and the detector. The particulates cause the electromagnetic waves to bounce and reflect in different directions. This has the effect of drastically decreasing the optical power that reaches the detector. Dust and smoke are examples of particulates responsible for scattering [2]. It is important to minimise the distance between the detector and source when performing Radiation Thermometry measurements.

Finally, the infrared light emitted from a Black Body is readily absorbed by the constituent gases of air. Each gas has a specific absorption spectra that will affect different sections of the Black Body spectrum [2]. Water Vapour and CO_2 are gases that absorb across large sections of the infrared spectrum. Specific frequency windows in the infrared spectrum have minimal absorption in air; it is possible to measure the optical power across these frequencies to provide a more accurate calculation of the object surface temperature [2].

4.3 Transimpedance Amplifiers

Transimpedance Amplifiers (TIA) are used to convert current-based input signals to voltage-based output signals. In their most basic form, they consist of an operational amplifier with a single feedback resistor from output to inverting input [6]. They are very commonly used to convert and amplify the signal produced by Photodiodes.

Unfortunately, Photodiodes introduce a small capacitance on the operational amplifier input. This forms a low pass filter with the feedback resistor, producing a second order response when the phase lag of the operational amplifier is accounted for [9]. To combat this, a sufficiently large feedback capacitor is introduced in parallel with the feedback resistor to produce a dominant pole in the amplifier frequency response. This results in the TIA producing a primarily first order response with a large phase margin from oscillation. A typical Photodiode TIA circuit with feedback capacitance can be seen in **Figure 4.2** [10].

From this schematic, we can derive **Equation 4** and **Equation 5** that describe the Transimpedance Gain and Corner Frequency of the Transimpedance Amplifier respectively [6].

$$\frac{V_{out}}{I_{in}} = -\frac{R_f}{j\omega C_f R_f + 1} \quad \Omega \tag{4}$$

$$\lim_{\omega \to 0} \frac{V_{out}}{I_{in}} = -R_f \quad \Omega$$

$$f_c = \frac{1}{2\pi C_f R_f} \quad Hz \tag{5}$$

As the Transimpedance Amplifier is the amplification stage connected to the Photodiode, it has the largest effect on improving the circuit's signal to noise ratio. Thus, it is worth focusing development efforts on producing a low noise Transimpedance Amplifier circuit for this project. Primarily, there are three types of noise to consider when developing TIAs: Johnson Noise, Shot Noise and Flicker Noise [6].

Johnson Noise, also known as Thermal Noise, is a noise generated by the thermal vibrations in resistors causing random collisions with travelling electrons [6]. It is a type of White Noise; this means it has a uniform power spectral density across its entire frequency spectrum. As the name suggests, Thermal Noise is Temperature dependent. **Equation 6** and **Equation 7** give the Johnson noise voltage spectral density and noise current spectral density respectively [6].

$$e_n = \sqrt{4kTR} \quad \frac{V}{\sqrt{Hz}} \tag{6}$$

$$i_n = \sqrt{\frac{4kT}{R}} \quad \frac{A}{\sqrt{Hz}} \tag{7}$$

Shot Noise is produced by fluctuations in the flow of electrons and is particularly prevalent at potential barriers, such as those generated by PN junctions [6]. The shot current noise spectral density can be calculated using **Equation 8**[4] [6].

$$i_n = \sqrt{2qI_{dc}} \quad \frac{A}{\sqrt{Hz}} \tag{8}$$

Flicker Noise is produced via various areas of the construction of electronic components, for example the material used for resistors or the metal end cap connections on surface mount components [6]. Flicker Noise is referred to as $1/f$ noise as the power spectrum approximately follows a $1/f$ curve, with the voltage and current spectrums following a $1/\sqrt{f}$ curve [6]. Unfortunately, as the power spectral density is highest at DC, flicker noise can drastically reduce the sensitivity of Photodiode circuits by increasing their noise floor [6].

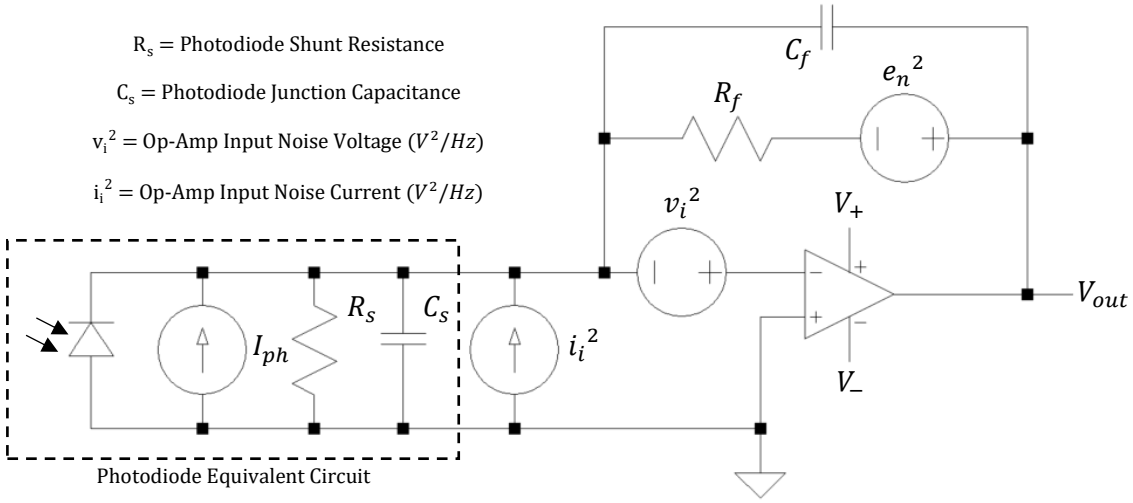

Figure 4.2: Transimpedance Amplifier Noise equivalent circuit

Figure 4.2 shows the equivalent noise circuit for a Transimpedance Amplifier [9] used with a Photodiode; this schematic highlights a few key decisions. Firstly, an operational amplifier with a small input noise current should be selected for TIA applications [6]. This noise current will be directly amplified by the TIA and will have a large effect on the circuit's signal to noise ratio.

Secondly, an operational amplifier with a small input noise voltage should be selected. The input noise voltage produces a noise current with the operational amplifiers input capacitance which is also amplified by the TIA [6].

Thirdly, an operational amplifier with a low flicker noise should be selected. As we are operating at DC this is very important [6].

Finally, as we are operating at DC we should use as high a value of R_f as possible [6] [11]. Performing a Thevenin to Norton conversion on the R_f noise model shows that the noise current will be amplified by the TIA. The resulting noise voltage will be much larger than that of R_f. This has the benefit of increasing the TIA gain, at the expense of bandwidth [11].

[4] Shot noise calculations assume all electrons are flowing independently of each other.

4.4 Voltage Amplifiers

Voltage Amplifiers (VAS), as the name suggests, perform a Voltage to Voltage amplification. The signal produced by the Transimpedance Amplifier will require further amplification; most modern Lock-in Amplifier ICs require an input signal in the order of *mV* to operate correctly. Two basic forms of Voltage Amplifier exist: Inverting and Non-Inverting [6].

For an Inverting Amplifier, we can derive **Equation 9** that gives the gain of the circuit assuming a very large Gain Bandwidth. Additionally, we can use **Equation 10** to calculate the potential Bandwidth for a given Gain and operational amplifier Gain Bandwidth [6].

$$\frac{V_{out}}{V_{in}} = -\frac{R_2}{R_1} \tag{9}$$

$$f_c = GBW \times \frac{V_{out}}{V_{in}} \quad Hz \tag{10}$$

For a Non-Inverting Amplifier, we can derive **Equation 11** that gives the gain of the circuit assuming a very large Gain Bandwidth [6]. Again, **Equation 10** gives the potential Bandwidth for a given Gain and Gain Bandwidth.

$$\frac{V_{out}}{V_{in}} = \frac{R_1 + R_2}{R_2} \tag{11}$$

To maintain an acceptable Signal to Noise ratio we must ensure that the Voltage Amplification stages used in the final design are low noise. There are several steps to achieve this. Firstly, an operational amplifier with a small input noise voltage must be selected [6]. Any noise on the input will be amplified by the VAS. Secondly, an operational amplifier with a small input offset voltage must be selected. Any DC offset introduced by the amplifier will be interpreted as a signal by the Lock-in Amplifier [6]. Finally, the lowest values available should be used for resistors R_1 and R_2. Limiting the resistance value will reduce the Johnson noise voltage introduced by the resistors.

Unfortunately, decreasing the resistance values comes with a trade-off for the Inverting Amplifier. As its input impedance is defined by R_1, this value must be kept high to avoid loading effects on previous sections of the circuit. However, the Inverting Amplifier circuit comes with the added benefit of a Gain equation that produces round values more easily with common resistor values.

4.5 Lock-in Amplifiers

As discussed in **Section 2,** Lock-in Amplifiers (LIA) are devices capable of extracting a modulated signal from a noise floor of 100*dB* and upwards [6]. They achieve this level of performance using a technique called Phase Sensitive Detection [4], a technique comparable to the process used in super heterodyne receivers for communication electronics.

A reference signal, usually a sine or square wave, is used to modulate the signal to be measured. An example of this modulation is the optical chopper discussed in **Section 2;** this produces a square wave modulation. The modulated input signal is then multiplied by the reference signal [4]. When a square wave reference is used, this produces a signal at DC and several harmonics of the reference frequency. The mathematical derivation for this is shown in **Appendix A**.

Passing the output signal from the multiplier through a Low Pass Filter produces a DC voltage proportional to the amplitude of the input signal [4], [6]. **Equation 12** shows the mathematical relationship between input signal and output voltage.

Ideally, the reference signal should be in phase with the input signal. Thus, most Lock-in Amplifiers incorporate a Phase Locked Loop (PLL) into their design [4]. The PLL can be omitted if the Reference Signal is used to drive modulation. A systems diagram for Phase Sensitive Detection is shown in **Figure 4.3**.

$$Output\ DC\ Signal \approx \frac{664 V_S V_R}{75\pi^2} \tag{12}$$

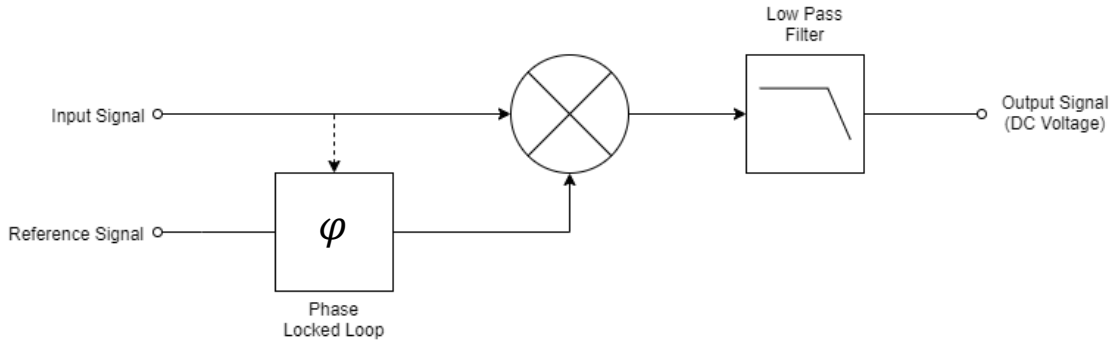

Figure 4.3: Phase Sensitive Detection Systems Diagram

Additionally, due to the Low Pass Filter on the output of the Lock-in Amplifier, the system imposes a form of Bandwidth Narrowing. This can aide in the systems overall noise performance by removing high frequency harmonics from the output signal [6]. As we are using the DC component of the multiplier output, only noise introduced by DC offsets will be present in the output signal.

The noise performance of a Lock-in Amplifier is known as the Dynamic Reserve; this is a measure of the scale factor between the signal amplitude and noise amplitude that the Lock-in Amplifier can still measure at [4]. As stated previously, modern Lock-in Amplifiers can achieve a Dynamic Reserve of 100*dB* and upwards [6]. **Equation 13** shows the calculation for Dynamic Reserve.

$$Dynamic\ Reserve\ (dB) = 20\log_{10}\left(\frac{V_{noise(RMS)}}{V_{signal(RMS)}}\right) \tag{13}$$

5 Methodology

This section briefly covers the thought processes and decisions made during the development of the Electronic Lock-in Amplifier. Based upon the theory discussed in **Section 4**, components were selected for the Transimpedance Amplifier, Voltage Stages, Lock-in Amplifier and Digital Conversion sections of the circuit board. This development has the aim of producing a Lock-in Amplifier circuit with as high a Signal to Noise ratio as possible; the higher the Signal to Noise ratio, the lower the amplitude of Photodiode signal that can be measured.

5.1 Photodiode Selection

As stated in **Section 4.3**, it is important to ensure the junction capacitance of the Photodiode is as small as possible in order to prevent oscillation in the Transimpedance Amplifier [6]. The junction capacitance is available on the datasheet of most Photodiodes.

It is also beneficial to select a Photodiode that will produce an output signal in the order of *nA*. The larger the output signal, the lower the Black Body temperature that can be measured. Consequently, a Photodiode with as large a sensitive area as possible should be selected. Unfortunately, an increase in sensitive area causes a proportional increase in junction capacitance [12]. Thus, we must select a Photodiode that produces an appropriate trade-off between junction capacitance and sensitive area. This situation is helped by selecting a Photodiode that is sensitive to as much of the Black Body frequency spectrum as possible.

Finally, a Photodiode with a low dark current should be selected. Dark current is the current produced by a Photodiode under no light (due to thermal excitations of electron hole pairs) [12], it acts as a noise floor for the Photodiode, limiting the minimum optical power that can be measured [12]. Theoretically, the dark current contribution to the signal noise should be removed by the Lock-in Amplifier. However, differences in Photodiode devices due to manufacturing tolerances mean that it is beneficial to limit the dark current where possible (discussed further in **Section 5.6**).

Component Name	Dark Current (*nA*)	Radiant Sensitive Area (mm^2)	Operating Wavelength Range (*nm*)	Peak Spectral Sensitivity (*A/W*)	Capacitance (*pF*)
SFH 2200	1	7.02	300 - 1100	0.7	60
BP 104 FS-Z	2	4.84	800 - 1100	0.7	48
RPMD-0100	0.5	1.8	800 - 1050	-	1.5
BPW 34 FS-Z	2	7.02	780 - 1100	0.7	72
VBPW43S	2	7.5	430 - 1100	-	70
SFH 2201	1	8.12	300 - 1100	0.7	65
S2386-5K	0.002	5.76	320 - 1100	0.6	730

Table 5.1: Candidate Photodiodes for the Electronic Lock-in Amplifier Circuit

Table 5.1 shows a set of candidate Photodiodes for the Electronic Lock-in Amplifier circuit. Based upon the trade-offs discussed above, the SFH 2200 [13] was selected as a good balance between Junction Capacitance, Dark Current and Sensitive Area.

5.2 Operational Amplifier Selection – TIA

As discussed in **Section 4.3**, it is important to ensure that the Transimpedance Amplifier contributes as little noise as possible to the signal. Therefore, we must ensure the operational amplifier used in the TIA has as low an input noise current, input noise voltage and flicker noise as possible. A CMOS or JFET input operational amplifier would be best placed to achieve this [6].

Furthermore, it will be beneficial to select an operational amplifier with a high Gain Bandwidth. In addition to improving the signal to noise ratio by maximising the gain on the first stage, a high gain is required to ensure the signal is large enough to be measured by the Lock-in Amplifier IC. As a Photodiode outputs signals in the range of *pA* to *nA* and the LIA IC requires signals in the order of *mV*, the circuit should be capable of an overall gain of approximately 10^9 before the LIA IC.

Finally, as square wave modulation is being used, a high Slew Rate operational amplifier may be useful if an amplification stage is placed after the modulation stage of the system.

Component Name	GBW (*MHz*)	Slew Rate (*V/μS*)	Input Noise Current ($pA/Hz^{1/2}$)	Input Noise Voltage ($nV/Hz^{1/2}$)	Input Offset Voltage (*μV*)	Cost (£)
OPA657	1600	700	0.0013	4.8	250	10.16
AD8065	145	180	0.0006	7	1500	3.20
AD795	1.6	1	0.0006	9	500	7.53
LMH6609	260	1400	1.6	3.1	2500	2.45
AD8628	2.5	1	0.005	22	5	3.04

Table 5.2: Candidate Operational Amplifiers for the Transimpedance Amplifier circuit

Table 5.2 shows some candidate operational amplifiers based upon the requirements listed above. In order to properly assess the suitability of each IC a series of simulations were performed using LT Spice [10].

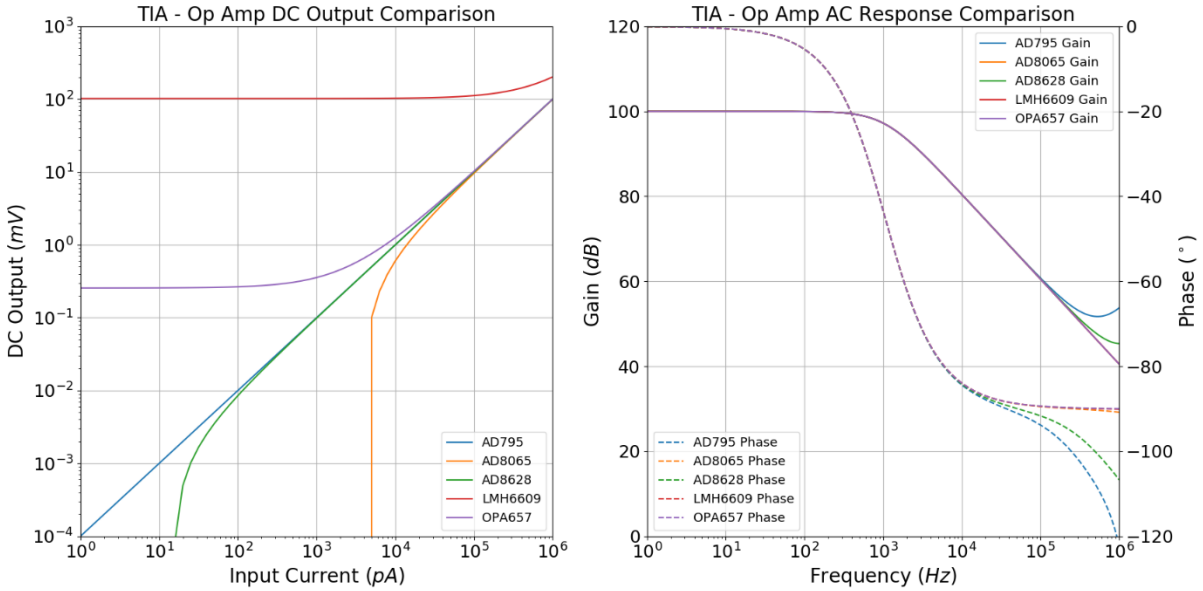

Figure 5.1: TIA Operational Amplifier - Sensitivity and AC Response Simulation Results

Figure 5.1 (right) shows the simulated frequency response of the candidate operational amplifiers. A feedback resistance (R_f) and capacitance (C_f) of 100*kΩ* and 1.5*nF* were selected to produce a TIA with a gain of 100k and a bandwidth of 1kHz. These values were calculated using **Equations 4** and **5**. This simulation shows that all candidate operational amplifiers can meet this specification.

Figure 5.1 (left) shows the simulated DC response of the candidate operational amplifiers. The AD795 exhibits the desired response of a linear response across the full input current range. The other amplifiers exhibit an output DC offset, with the AD8628 performing closest to the AD795. This DC offset is produced by the combination of noise sources on the amplifier input and the operational amplifier input bias current.

Figure 5.2 shows the simulated output noise response of the candidate operational amplifiers. Again, the AD795 and AD8628 produce the best performance with noise voltages below $120nV/Hz^{1/2}$ across the full frequency spectrum. The effects of flicker noise are also shown, particularly by the LMH6609 and AD8065, by the increase in noise voltage spectral density as the frequency tends to 0.

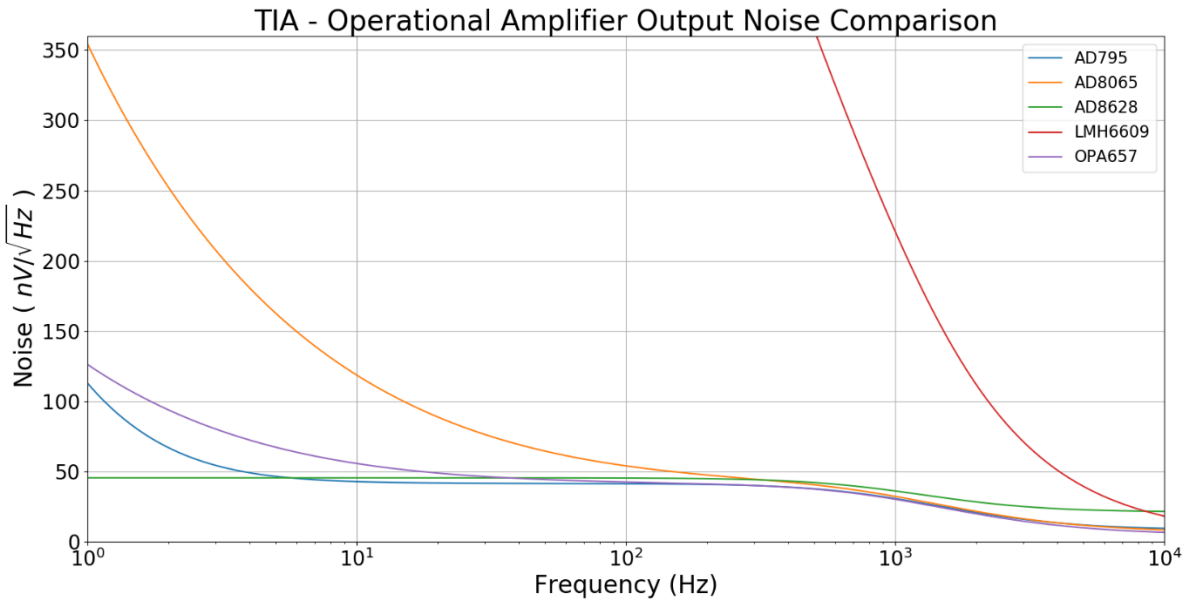

Figure 5.2: TIA Operational Amplifier Output Noise Simulation Results

It is important to note that, as the above results are based upon simulations, they cannot be taken as the absolute truth. The SPICE models provided for each operational amplifier will have varying levels of complexity and accuracy through the number of effects (temperature, flicker noise, etc.) they model.

Based upon the information above, the AD795 [14] and AD8065 [15] were selected for further practical investigation as candidates for the Transimpedance Amplifier design. The AD795 has been selected for its low noise characteristics and exceptional linearity, at the expense of higher cost and lower gain bandwidth. The AD8065 has been selected as a low-cost alternative with comparable noise performance and the added benefit of greater gain bandwidth. This is part of an attempt to limit the total BOM cost of the Lock-in Amplifier where possible.

5.3 Operational Amplifier Selection – VAS

As discussed in **Section 4.4**, it is important to select a low noise operational amplifier for the Voltage Amplification Stage (VAS) in order to minimise the effect on the circuit signal to noise ratio. Therefore, we must ensure that the operational amplifier has as low an input noise voltage and input offset voltage as possible. Additionally, as outlined in **Section 5.2** it will be beneficial to select an operational amplifier with a high slew rate.

To provide simpler calculations for the Voltage Stage gain, an Inverting Amplifier configuration was selected. Resistors R_1 and R_2 were given values of 10Ω and $1k\Omega$ respectively; this attempts to minimise the Johnson noise contribution from the resistors and gives a gain of 100.

Table 5.3 shows some candidate operational amplifiers based upon the requirements listed above. In order to properly assess the suitability of each IC further simulations were performed using LT Spice [10].

Component Name	GBW (*MHz*)	Slew Rate (*V/μS*)	Input Noise Voltage ($nV/Hz^{1/2}$)	Input Offset Voltage (*μV*)	Cost (£)
LTC6078	0.75	0.05	18	7	3.315
OPA827	22	28	4	75	7.94
LT1007	8	2.5	2.8	10	4.10
LT1677	7.2	2.5	3.2	35	4.175
LMP2021	5	2.6	11	-0.4	2.23

Table 5.3: Candidate Operational Amplifiers for the Voltage Amplification Stage circuit

Figure 5.3 (right) shows the frequency response of the candidate operational amplifiers with the Inverting Amplifier configuration discussed above. As large a bandwidth as possible would be beneficial in the event a Voltage Amplification Stage is placed after the Lock-in Amplifier modulation circuitry. Consequently, the LTC6078 is removed from the selection process as it has a significantly lower bandwidth than the other amplifiers in this configuration.

Figure 5.3 (left) shows the simulated DC response of the candidate operational amplifiers. The LT1007 and LT1677 exhibit the desired linear response, making them good candidates for this application. The OPA827 and LMP2021 both have a slightly negative offset on their output voltage, leading to a negative output at very low input voltages. Hence, as **Figure 5.3 (left)** is a log-log scale graph, they exhibit an extreme roll off. They are also good candidates for this application.

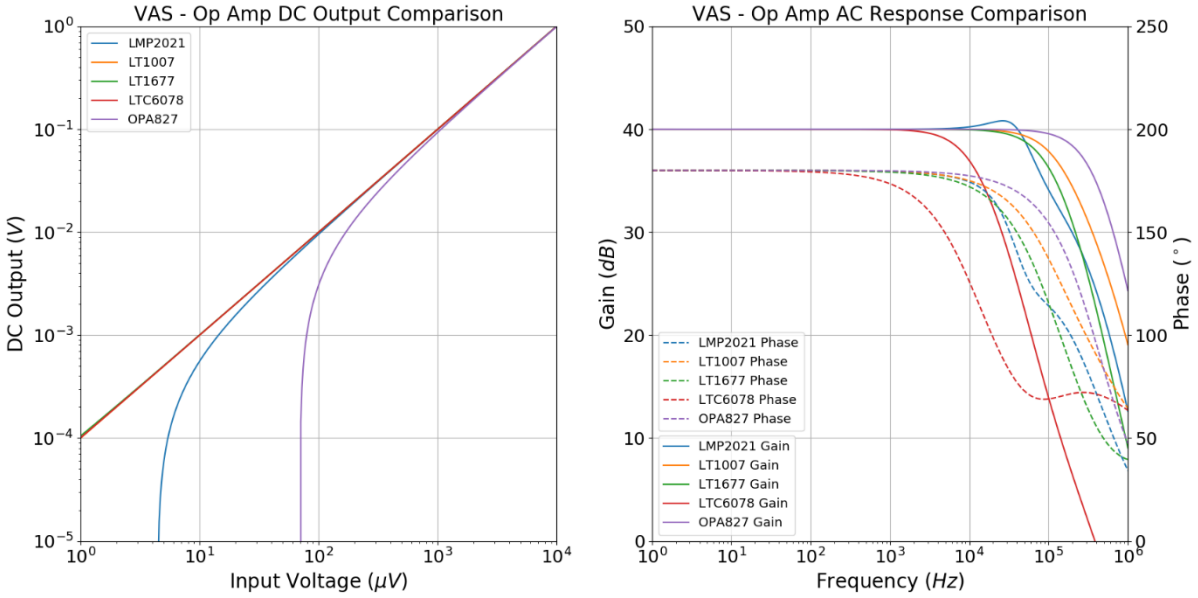

Figure 5.3: VAS Operational Amplifier Sensitivity and AC Response Simulation Results

Figure 5.4 shows the simulated output noise response of the candidate operational amplifiers. The LT1007 shows the best performance with an output voltage noise spectral density below $50nV/Hz^{1/2}$ across the entire frequency spectrum. The OPA827 and LT1677 are also good candidates with an output noise voltage spectral density below $2\mu V/Hz^{1/2}$ across the entire frequency spectrum. Again, the effects of flicker noise are also exhibited, as the noise voltage spectral density increases as the frequency trends towards zero.

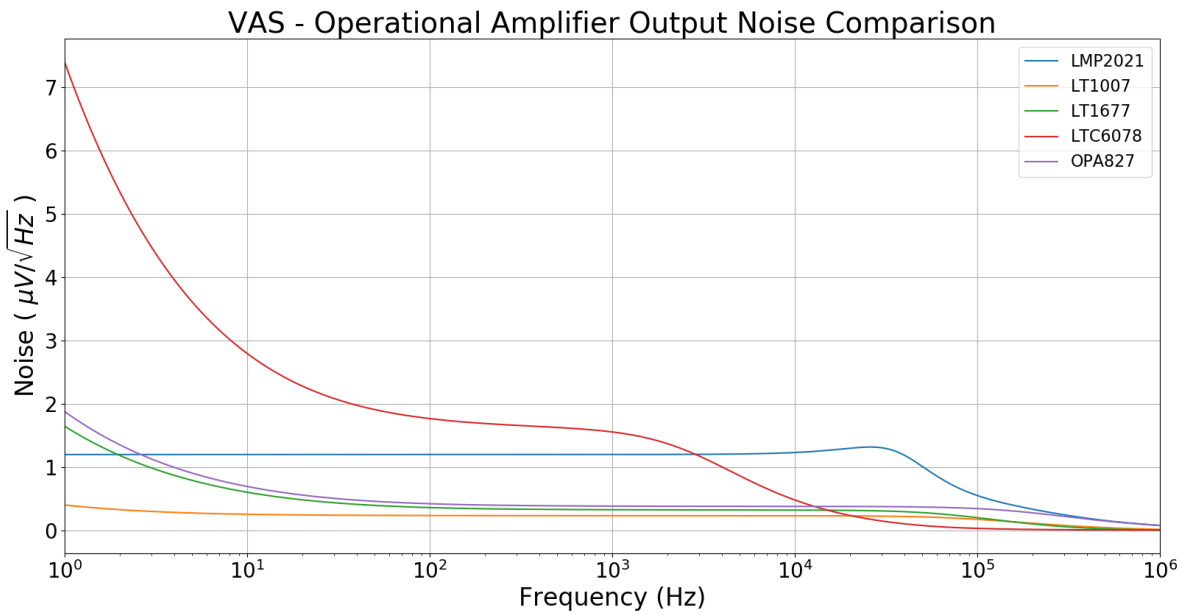

Figure 5.4: VAS Operational Amplifier Output Noise Simulation Results

Based upon the above results, the LT1007, LT1677 and OPA827 are all good candidates for the VAS. As the LT1007 [16] exhibited the best simulated output noise performance it was selected for further practical testing. Additionally, the OPA827 [17] was selected as a back-up IC due to its greater Gain Bandwidth.

5.4 Analogue Switch Selection

The Analogue Switch will be used in place of the Optical Chopper discussed in **Section 2** to perform the modulation of the input signal to the Lock-in Amplifier IC. As it is in the signal path, it must meet some key requirements: low On-State resistance, low Off-State leakage current, low channel cross talk, fast switching times and break before make operation.

The low On State resistance, Off State leakage current and channel cross talk ensure that the switch does not attenuate the input signal, introduce an additional noise contribution via a leakage current producing a DC offset or allow the input signal to introduce noise in the reference signal. Additionally, fast switching times allow for a high reference signal frequency should it be required. Finally, the break before make operation ensures the input and reference channels will not short momentarily.

Per the above requirements, the ADG849 was selected as the Analogue Switch for the Lock in Amplifier circuit. This IC has an On-State resistance of 0.5Ω, an Off-State leakage current of 0.4*nA*, -64*dB* of channel cross talk and can switch at 40*MHz*; this makes it sufficient for the circuit's requirements.

5.5 Lock in Amplifier IC Selection

Analysis of the Lock in Amplifier circuit design by Tarick Osman [8] indicates that the AD630 used in the design provides a convenient package specifically designed for Phase Sensitive Detection. This not only makes PCB design easier; it also removes complexity from the design process by providing near black box functionality for the Phase Sensitive Detection section of the circuit. Unfortunately, the AD630 limits the sensitivity of the circuit to the 10s of *nA* due to its input offset voltage and the sensitivity of its inputs (requiring signals in the *mV* range) [8]. The increased gain of the new design aims to alleviate these problems by amplifying *nA* signals to 10s of *mV* before the LIA IC.

The AD630 has now been discontinued by Analog Devices. A replacement IC, the ADA2200 [18], has been introduced. The ADA2200 uses digital techniques to perform Phase Sensitive Detection, as opposed to the fully analogue implementation of the AD630. This digital implementation provides additional functionality such as programmable filters and an internally generated reference signal [18]. To simplify the design process whilst ensuring a maintainable design, the ADA2200 has been selected as the LIA IC for this circuit.

5.6 Complete Circuit Design

Following the design decisions discussed above, a schematic for the Lock in Amplifier circuit was produced using the open source schematic and PCB design software KiCAD [19]. This schematic is shown in **Appendix C**.

Initially, both of the designs discussed in **Section 5.2** and **Section 5.3** were used for the TIA and VAS stages of the circuit. Following practical testing component values were changed to provide better performance (discussed further in **Section 6.2**), the schematics shown in **Appendix C** are the final versions. In addition to the Inverting Amplifier design discussed in **Section 5.3**, the first VAS stage also has provision for a Non-Inverting Amplifier configuration allowing for smaller values of overall gain.

Building upon the analysis completed by Tarick Osman [8], a split amplifier configuration has been used. This has been extended so that each Photodiode has a unique chain of three amplifiers, one Transimpedance Amplifier and two Voltage Amplification Stages. This allows the modulation stage to be placed after all the amplification; consequently, much higher reference signal frequencies can be used. This will allow for experiments to ascertain the best value of reference signal frequency. Testing signals can be input to the circuit using connectors J1 and J2. The output of the Transimpedance Amplifiers can be measured using connectors J3 and J4.

The reference signal for the analogue switch used in the modulation stage (U10) is provided by the Lock-in Amplifier IC directly, as discussed in **Section 5.5**. This reference signal is multiplexed by U4 as the reference pin on the ADA2200 is also used for SPI communications [18]. This reference signal can be measured using connector J9.

The ADA2200 has been configured as per the guidance provided in the datasheet for a Lock-in Amplifier application [18]. Connections for both SPI and I2C communication have been implemented, allowing for greater flexibility in software. Serial communication with the ADA2200 allows for control of the programmable filter [18]. Three low pass filter configurations are implemented to allow for different corner frequencies of $1.6Hz$, $0.16Hz$ and $0.016Hz$; thus, a wider range of reference signal frequencies can be used. The ADA2200 sync out pin has also been connected to the microcontroller; this allows the software to trigger an ADC read when the output of the LIA is stable [18]. Connectors J6, J7 and J8 allow the LIA IC to be bypassed for testing purposes.

To improve the granularity of the digital measurement of the Lock-in Amplifier output over the previous design, a standalone ADC was implemented (U7). The AD7171 [20] was selected as it provides 16-bit conversion at a low cost. 16 bits gives a resolution of $50.35\mu V$ across a $3.3V$ range. An ADR381 analogue reference has also been implemented to support the AD7171 [21].

A Teensy 3.2 [22] has been selected as the microcontroller for the design. This development board provides a 32-bit Cortex-M4 processor, clocked at $72MHz$. This high clock speed should allow for Digital Signal Processing techniques to be applied to the Lock-in Amplifier output signal, should they be required. Several serial interfaces are provided, allowing for future expansion of the circuit design

should it be required. The Teensy 3.2 is programmed using Arduino, giving a much simpler and faster programming experience.

For convenience, an LM2937 linear voltage regulator [23] has been added to provide the 3.3*V* power supply rail of the circuit. Over-voltage protection Zener diodes have also been placed on the 5V rails.

Finally, a set of three tactile switches and connections for an LCD display have been provided. This should allow for the implementation of a simple user interface for the Lock-in Amplifier, allowing for easier measurements and calibration routines (should they be required).

5.7 PCB Design

Upon completion of schematic design, the physical layout of the PCB could be completed using KiCAD [19]. The main aim of the design is to minimise the noise introduced in the analogue section of the circuit, both due to external sources and other sections of the PCB (for example, the digital switching and power supply sections). A 3D render of the completed PCB layout is shown in **Appendix D**.

Bypassing capacitors of 100*pF* and 100*nF* have been placed as close as possible to the power supply pins of all Integrated Circuits to negate the effects of power supply ripple. Additionally, a 10μF capacitor has been placed across the 5V and -5V lines to further smooth the power supply lines [24].

The circuit has been split into two key sections, Analogue and Digital. Both sections are kept physically apart where possible [24]. Additionally, a split ground plane has been implemented, with one connection at the input power connector. This is based upon the guidance given in the AD7171 datasheet [20]; it aims to limit the interference caused by switching digital signals on the sensitive analogue electronics by providing separate ground paths. The ground plane is placed on both the top and bottom side of the PCB; each side is connected through regularly spaced vias that aim to limit stray inductance in the ground plane by reducing ground loops [24].

Where possible, all analogue components were placed close together to limit trace lengths, thus limiting parasitic capacitance and inductance [24]. Digital and analogue traces on either side of the board were run perpendicular to each other to limit inductive coupling.

When selecting component footprints, the most commonly available were chosen to increase the flexibility of the design. This allows for operational amplifiers and switches to be changed more easily. All passive components are implemented in the 1206 SMD size to make hand assembly of the PCB more manageable.

Finally, test points were connected to all key signals to facilitate debugging and connection to test equipment.

5.8 TIA and VAS Testing

In order to verify the operation of the Transimpedance Amplifier and Voltage Amplification Stage designs a set of practical tests were performed to replicate the simulations in **Section 5.2** and **5.3.**

Frequency response tests were performed using the setup shown in **Appendix B.** A Function Generator provided a 100*mVpp* Sine wave swept from 1*Hz* to 100*kHz* as an input signal for the prototype TIA and VAS circuits. An Oscilloscope was used to take measurements of Phase, Input Voltage (RMS) and Output Voltage (RMS). To mimic a current source on the TIA input, a large value resistor (1$M\Omega$ to 1$G\Omega$) was placed in series with the input [25].

Sensitivity tests were performed using a Function Generator and Stanford Research Systems SR830 Lock-in Amplifier. A 200*Hz* Sine wave between 200*mV*[5] and 5*V* was used as an input signal. The input signal was split, allowing it to also be used as the LIA reference. Again, to mimic a current source, a large value resistor was placed on the TIA input. This allowed for very small values of current (10*pA* to 100*nA*) to be generated. To produce signals in the *µV* range, a potential divider was used on the VAS input.

Output noise tests were performed by connecting the output of a powered TIA to a Stanford Research Systems SR760 Spectrum Analyser with no input signal. At present, output noise tests have not been performed for either of the VAS designs.

5.9 Black Body Radiation Testing

To ascertain the performance of the previous Lock-in Amplifier design [8] for Radiation Thermometry applications, a test setup was created using an Infrared Systems Development IR-301 controlled Black Body source, on an optical table. A 50*mm* focal length lens was used to focus light from the Black Body source onto the sensing BPX65 Photodiode. The reference Photodiode was covered by black tape.

The temperature of the Black Body source was then swept downwards from 1000°C in 100°C steps, 30 minute intervals were given between each step to allow the temperature of the source to settle and equilibrate. At each temperature step the analogue output of the Lock-in Amplifier was measured using a Multimeter. An image of the Black Body testing setup is shown in **Appendix E**.

6 Results and Analysis

This section outlines the results of the testing setups discussed in **Section 5.8** and **Section 5.9**. Results from this testing indicate the validity of the designs used in the Lock-in Amplifier circuit, any changes that need to be made to the final schematic and inform on future work required by the project. An example of the circuit boards used for testing can be seen in **Appendix F**.

6.1 Transimpedance Amplifier Testing

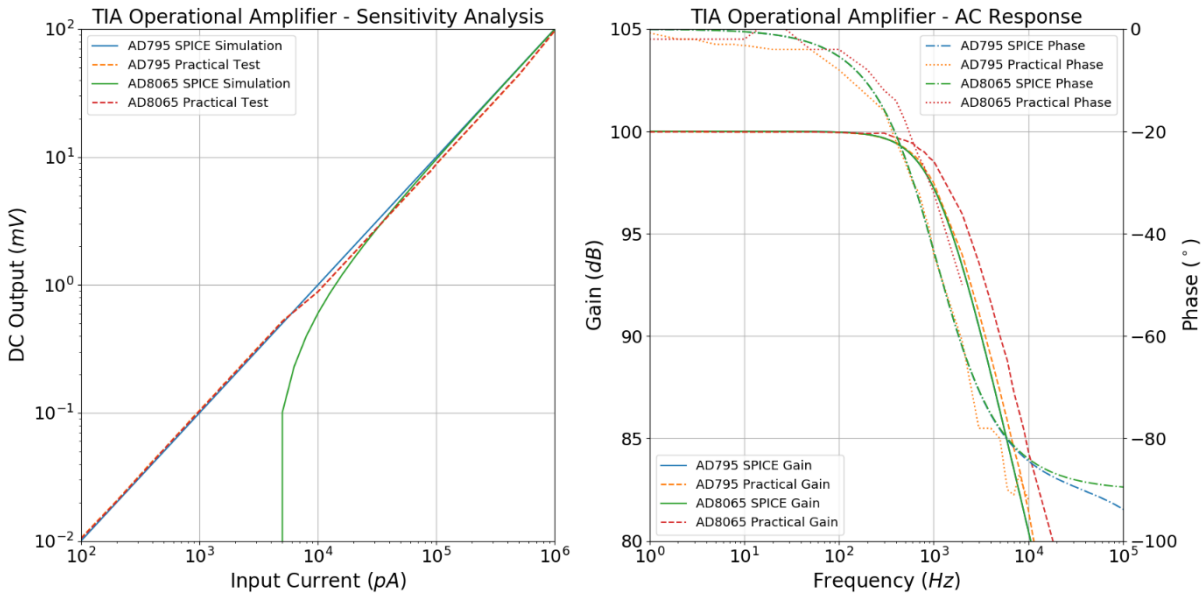

Figure 6.1: TIA Operational Amplifier - Sensitivity and AC Response Practical Results

[5] Signals below 200*mV* cannot be detected by the SR830 Reference input.

Figure 6.1 (right) shows the results from the AC response testing of the Transimpedance Amplifier configurations discussed in **Section 5.2**. This graph clearly shows that both the AD795 and AD8065 meet the frequency response requirements of 100*dB* Passband Gain and a Corner Frequency of 1*kHz*. It is important to note the difficulty in measuring the phase at frequencies above 1*kHz* was due to the attenuation of the output signal.

Figure 6.1 (left) shows the results from the Sensitivity testing of the Transimpedance Amplifier configurations. Both operational amplifiers have a linear response down to 100*pA*, a signal lower than the dark current of most Photodiodes. The small shifts in the practical data are due to changes in the series resistor value used to generate the input current. As stated in **Section 5.2**, the roll off in the AD8065 simulation result is due to a negative offset on the output of the amplifier; this is not shown in the practical results. Both operational amplifiers meet the sensitivity requirements of the LIA design.

Unfortunately, due to the similarity in noise curves, the results from the output noise experiments are inconclusive. Both curves have much higher noise than expected at low frequencies and overlap at high frequencies. At present, these results indicate that the amplifiers noise is below the noise floor of the Spectrum Analyser. Further testing is required to ascertain whether this is correct and to obtain a correct noise spectral density curve for each operational amplifier.

Both the AD8065 and AD795 are suitable candidates for the Transimpedance Amplifier design due to their performance on both the AC and Sensitivity analysis tests. However, further testing is required to properly characterise the noise spectral density characteristics of each amplifier. As the AD8065 is a lower cost operational amplifier, it will be the first option for future testing of the Lock-in Amplifier design.

6.2 Voltage Amplification Stage Testing

At present, practical testing has only been completed on the LT1007 as a candidate for the Voltage Amplification Stage operational amplifier. As such, comparisons cannot be drawn between the LT1007 and OPA827 with the current results. However, the following testing results will indicate the suitability of the LT1007 for future testing of the Lock-in Amplifier design.

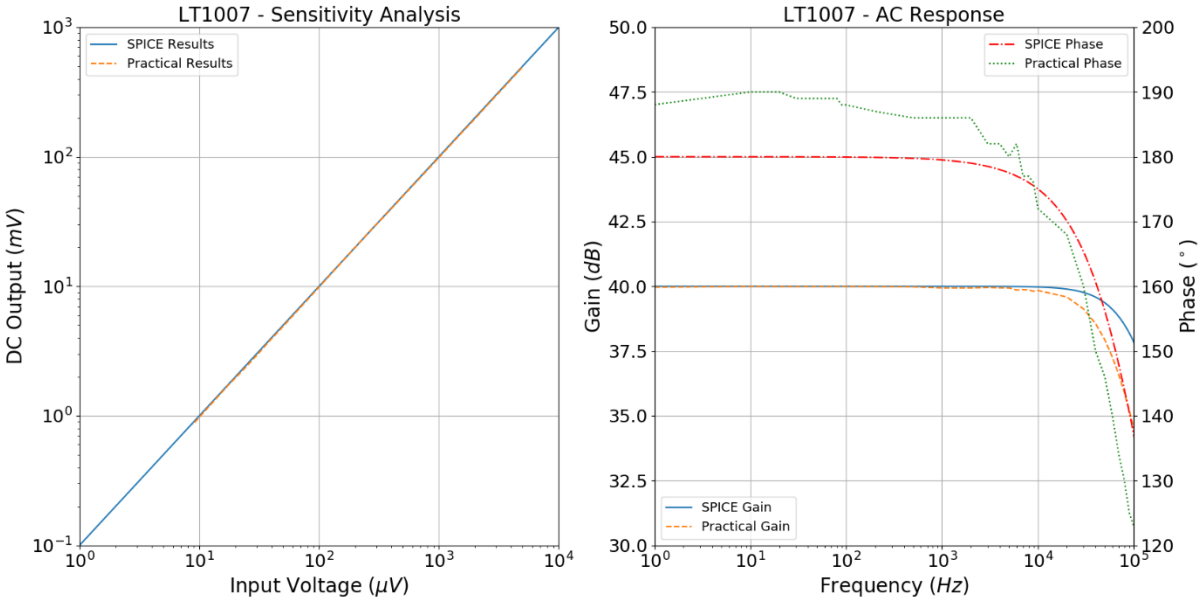

Figure 6.2: VAS Operational Amplifier - Sensitivity and AC Response Practical Results

Figure 6.2 (right) shows the practical AC response results for the LT1007 operational amplifier. The bandwidth of the practical amplifier is lower than the simulated result, with a value of approximately 2*kHz*. However, this value is still acceptable as it can easily match the Transimpedance Amplifier bandwidth of 1*kHz*. The amplifier has also correctly reached the desired gain of 40*dB*.

Figure 6.2 (left) shows the practical Sensitivity analysis results for the LT1007 operational amplifier. The LT1007 exhibits a perfectly linear response down to 10μV, making it a suitable candidate for the Voltage Amplification stage.

The LT1007 is a suitable candidate for the Voltage Amplification stage. As it is less expensive than the OPA827, it will be the primary candidate for future practical testing. It is important to note that during testing resistors R_1 and R_2 were increased to 1$k\Omega$ and 100$k\Omega$ respectively. This increased the input impedance, negating the initially observed loading on the Function Generator.

6.3 Lock-in Amplifier Radiation Thermometry Testing

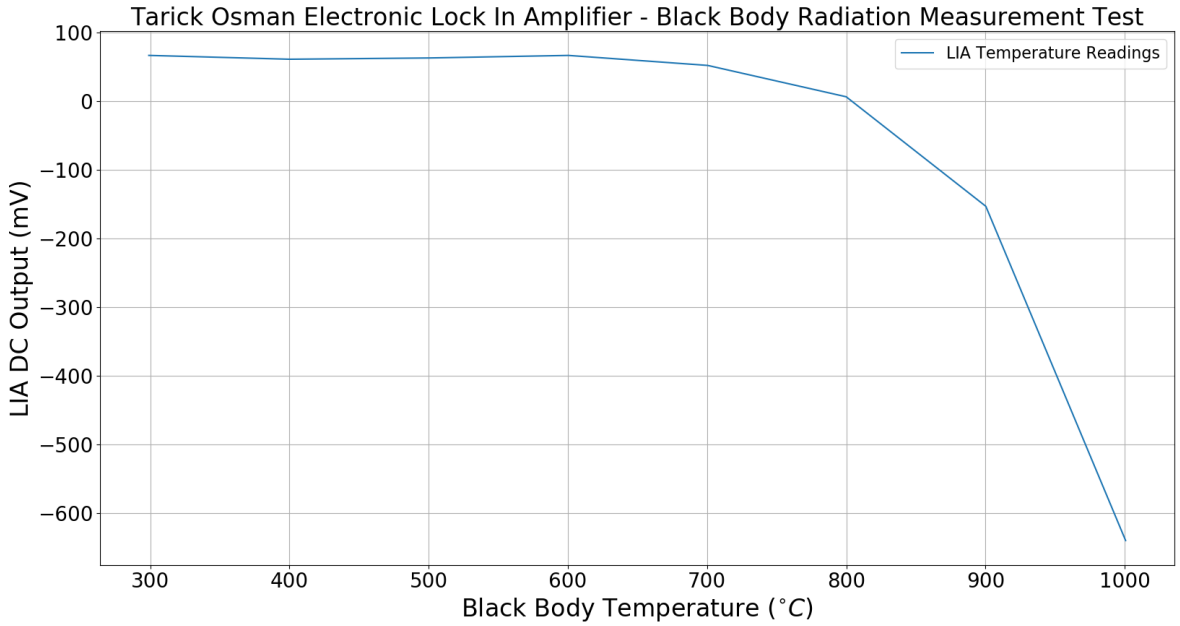

Figure 6.3: Radiation Thermometry Testing using LIA developed by Tarick Osman

Figure 6.3 shows the results of the testing outlined in **Section 5.9**. These results will act as a benchmark for future testing of the new Lock-in Amplifier circuit design. The graph indicates that the current Lock-in Amplifier design can only reliably measure down to a temperature of 700°*C*. The ideal temperature range of most Radiation Thermometers is 400 to 1000°*C*; thus, there is still considerable improvement to be made. The exponential shape of the graph is explained by **Equation 2** and **3**. Firstly, the total spectral radiance emitted by the Black Body decreases with temperature by a power of 4, leading to the curve shown above. Secondly, as the wavelength of peak intensity shifts to lower values with increasing temperature, the Black Body frequency spectrum will overlap with more of the Photodiode detection spectrum. This introduces further non-linearity into the measurement.

Ultimately, measuring a temperature lower than 700°*C* with the new Lock-in Amplifier circuit design will indicate an improvement in performance. However, due to the exponential nature of total spectral radiance, lower temperatures become much harder to measure.

7 Discussion and Conclusions

In conclusion, a new Lock-in Amplifier design has been developed and completed over the first term, including schematic design and PCB layout. This design incorporates Transimpedance Amplifiers and Voltage Amplification Stages that have been verified through simulation and practical testing; all significant results so far indicate that these designs are suitable for the task. Both the AD795 and AD8065 are suitable operational amplifiers for the TIA design, due to their frequency response and linearity, with the latter as the primary candidate due to its lower cost. The LT1007 is a suitable candidate for the VAS design due to its excellent linearity and frequency response.

Additional improvements have been made to the Lock-in Amplifier design including a 16-bit ADC, a more modern Lock-in Amplifier IC, higher performance analogue switch and greater overall gain capability before the LIA. The layout of the PCB has been optimised to decrease noise where possible; however, this is a proof of concept that has not been designed for manufacture or EMC compliance.

Finally, a Radiation Thermometry test of the previous Lock-in Amplifier design has been completed, at present this design can measure down to 700*°C.* This data acts as a benchmark for testing the new design, as well as indicating the validity of the basic concept.

Ultimately, definitive conclusions cannot yet be drawn about the performance of the new Lock-in Amplifier design. However, initial indications from practical testing are promising. Consequently, the project currently presents no major risks. This project aims to develop a low-cost Electronic Lock-in Amplifier solution for use in Radiation Thermometry applications. This should allow for more portable and affordable temperature measurement solutions, potentially allowing for safer and more efficient working environments by making high temperature measurement more accessible for small businesses and manufacturers. **Table 7.1** shows a price comparison between a current Lock-in Amplifier solution and the new design. As the current solution is 50 times the price of the new design, the low-cost element of the project has been met.

Component	Current Solution	Cost (£)	New Solution	Cost (£)
Lock-in Amplifier	SR830 Lock-in Amplifier	4190	Lock-in Amplifier	≈ 120
Modulation	SR540 Optical Chopper	1012		
	Total Cost (£):	5202	**Total Cost (£):**	≈ 120

Table 7.1: Current and New Lock-in Amplifier Solution Price Comparison

8 Milestone Evaluation

The Project Initialisation Document outlines a set of key milestones for the project. These milestones are as follows:

1) M1 ➔ Completed Low Noise High Gain TIA/LIA Circuit design.
2) M2 ➔ Completed Radiation Thermometry measurements and TIA/LIA PCB Design.
3) M3 ➔ TIA/LIA PCB Constructed.
4) M4 ➔ TIA/LIA PCB performance with Photodiodes tested.

From the work evidenced in **Section 5.2, 5.3, 5.6, 5.7, 6.1, 6.2** and **6.3**, both milestone 1 and 2 have been successfully completed during the first term of work. This complies with the Gantt chart shown in **Appendix G**, a modified version of the original chart shown in the PID.

One minor deviation from the original project schedule occurred over the first term. The development and testing of the TIA and VAS took an extra 2 weeks due to the setup and completion of tests taking longer than estimated. This postponed the completion of milestone 1 by two weeks. This change is reflected in **Appendix G**. Due to the very minor deviations from the project schedule and full access to departmental labs and equipment throughout the term, no risks were triggered from the risk register. Consequently, no changes have been made to the risk register document, which can be seen in **Appendix H**.

In addition to the Project Schedule, a few other techniques were employed to effectively manage the project. A Trello [26] board was created to manage subtasks and auxiliary tasks that needed to be completed to meet major milestones. Each task has a deadline set against it to aide with time management and planning for the week of work ahead. Additionally, a purchase order form was generated to keep track of project costs, an example of this can be seen in **Appendix I**. Finally, major meeting minutes were recorded with a word processor to properly capture any technical discussion.

9 Future Work

Based upon the development and results outlined above, the following future work should now be completed in order to achieve milestones 3 and 4:

- Additional testing should be completed on the Transimpedance Amplifier operational amplifier candidates to characterise their noise spectral density curve.
- Testing of the OPA827 as a candidate for the Voltage Amplification Stage design should be completed using the techniques described in **Section 5.8.**
- Additional Radiation Thermometry testing should be completed using the existing Lock-in Amplifier design to produce a more granular curve of output against temperature. Additionally, interfering sources of radiation should be used to ascertain how well the Lock-in Amplifier reduces noise and the optimal reference signal frequency.
- The Lock-in Amplifier PCB design outlined in **Section 5.7** has been sent for manufacture. Upon arrival of the manufactured PCB and components, the prototype PCB should be populated, visually inspected and tested using a pair of function generators.
- Upon completion of initial testing of the new Lock-in Amplifier design, further Radiation Thermometry tests should be performed using the new system to compare the two designs. This will categorically indicate whether an improvement has been made over the previous design.

10 References

[1] D. P. DeWitt, *Applications of Radiation Thermometry*. ASTM, 1985.

[2] P. Saunders, *Radiation Thermometry - Fundamentals and Applications in the Petrochemical Industry*. Bellingham, Washington 98227-0010 USA: SPIE, 2007.

[3] D. W. Ball, *Field guide to spectroscopy*. Bellingham, Wash.: SPIE Press, 2006.

[4] 'About Lock in Amplifiers'. Stanford Research Systems, Jan-2020.

[5] 'SR830 Lock in Amplifier Manual'. Stanford Research Systems, Oct-2011.

[6] P. Horowitz, *The Art of Electronics*, Third edition. New York, NY: Cambridge University Press, 2015.

[7] 'Stanford Research Systems SR810 and SR830 Lock in Amplifiers', *Stanford Research Systems*, Jan-2020. [Online]. Available: https://www.thinksrs.com/products/sr810830.html.

[8] T. Osman, 'Electronic Lock-In Amplifier for Measuring Low Optical Power', *Univ. Sheff.*, 2019.

[9] A. Auckloo, R. Tozer, J. David, and C. H. Tan, 'A low noise op-amp transimpedance amplifier for LIDAR applications', presented at the 21st IEEE International Conference on Electronics, Circuits and Systems (ICECS), NJ, 2014.

[10] Analog Devices, 'LT SPICE', *LT SPICE Design Center*, Jan-2020. [Online]. Available: https://www.analog.com/en/design-center/design-tools-and-calculators/ltspice-simulator.html.

[11] G. Giusi, G. Cannatà, G. Scandurra, and C. Ciofi, 'Ultra-low-noise large-bandwidth transimpedance amplifier: ULTRA-LOW-NOISE LARGE-BANDWIDTH TRANSIMPEDANCE AMPLIFIER', *Int. J. Circuit Theory Appl.*, vol. 43, no. 10, pp. 1455–1473, Oct. 2015, doi: 10.1002/cta.2015.

[12] J. Allison, *Electronic engineering semiconductors and devices*, 2nd ed. London ; New York: McGraw-Hill, 1990.

[13] O. Opto Semiconductors, 'SFH 2200 Datasheet'. 23-Jun-2017.

[14] Analog Devices, 'AD795 Operational Amplifier Datasheet'. Analog Devices, 2019.

[15] Analog Devices, 'AD8065 Operational Amplifier Datasheet'. Analog Devices, 2019.

[16] Linear Technology, 'LT1007 Operational Amplifier Datasheet'. Linear Technology.

[17] Texas Instruments, 'OPA827 Operational Amplifier Datasheet'. Texas Instruments, Jul-2016.

[18] Analog Devices, 'ADA2200 Synchronous Demodulator Datasheet'. Analog Devices.

[19] W. Stambaugh, 'KiCAD PCB Design Software', 2019. [Online]. Available: https://kicad-pcb.org/. [Accessed: 13-Jan-2020].

[20] Analog Devices, 'AD7171 Analogue to Digital Converter Datasheet'. Analog Devices, 2019.

[21] Analog Devices, 'ADR381 Analogue Reference Datasheet'. Analog Devices, 2019.

[22] PJRC, 'Teensy 3.2 Datasheet'. PJRC, 2019.

[23] Texas Instruments, 'LM2937 Linear Voltage Regulator Datasheet'. Texas Instruments, 2014.

[24] P. C. D. Hobbs, *Building electro-optical systems: making it all work*, 2nd ed. Hoboken, N.J: Wiley, 2009.

[25] L. Qiao, 'Methodologies for low excess noise measurement in wide bandgap materials', The University of Sheffield, 2017.

[26] Trello, 'Trello', 2020. [Online]. Available: https://trello.com/. [Accessed: 14-Jan-2020].

11 Appendices

Appendix A – Lock in Amplifier with Square Wave Reference Mathematical derivation

$$Square\ Wave\ Fourier\ Series = \frac{4}{\pi}\left(\sin(\omega t) + \frac{1}{3}\sin(3\omega t) + \frac{1}{5}\sin(5\omega t) + \cdots\right), \quad \omega = 2\pi f$$

$$Square\ Wave\ Fourier\ Series \approx \frac{4}{\pi}\left(\sin(\omega t) + \frac{1}{3}\sin(3\omega t) + \frac{1}{5}\sin(5\omega t)\right)$$

$$Input\ Signal\ (V_{sig}) \approx \frac{4V_s}{\pi}\left(\sin(\omega t) + \frac{1}{3}\sin(3\omega t) + \frac{1}{5}\sin(5\omega t)\right)$$

$$Reference\ Signal\ (V_{ref}) \approx \frac{4V_R}{\pi}\left(\sin(\omega t) + \frac{1}{3}\sin(3\omega t) + \frac{1}{5}\sin(5\omega t)\right)$$

$$V_{sig} \times V_{ref} \approx \frac{16V_sV_R}{\pi^2}\left(\frac{259}{450} - \frac{\cos(2\omega t)}{10} - \frac{2cost(4\omega t)}{15} - \frac{23\cos(6\omega t)}{90} - \frac{\cos(8\omega t)}{15} - \frac{\cos(10\omega t)}{50}\right)$$

Appendix B – Frequency Response Testing Setup

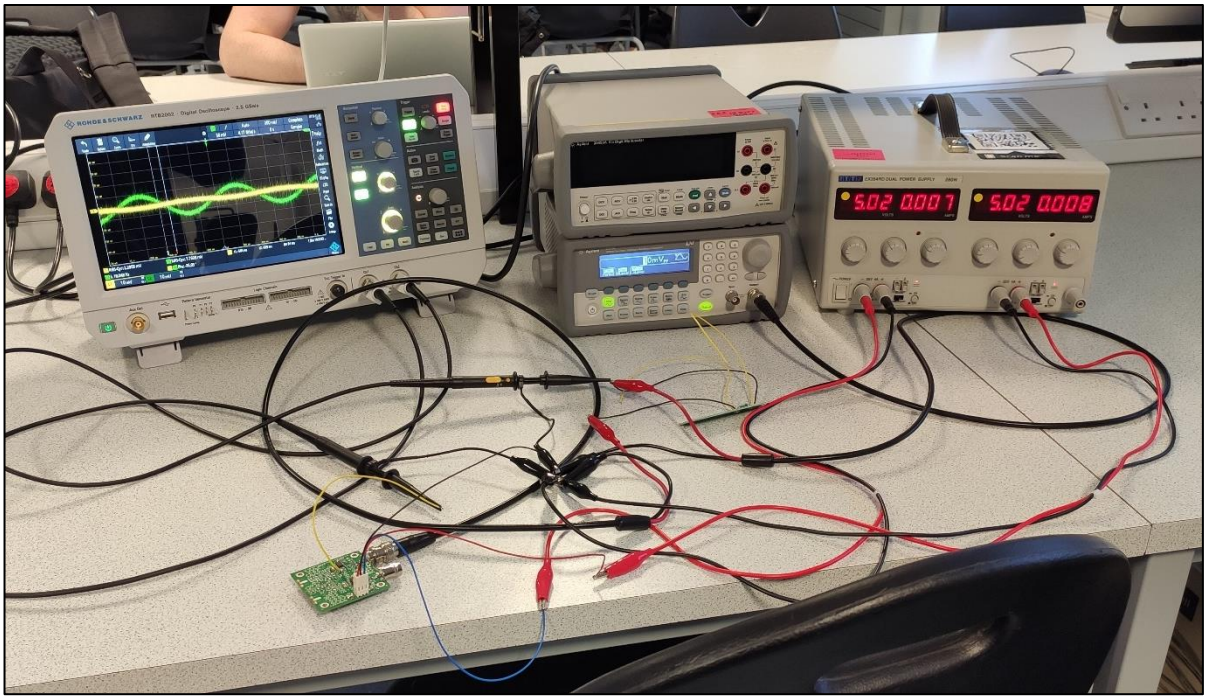

Appendix C – Completed Lock in Amplifier Schematic

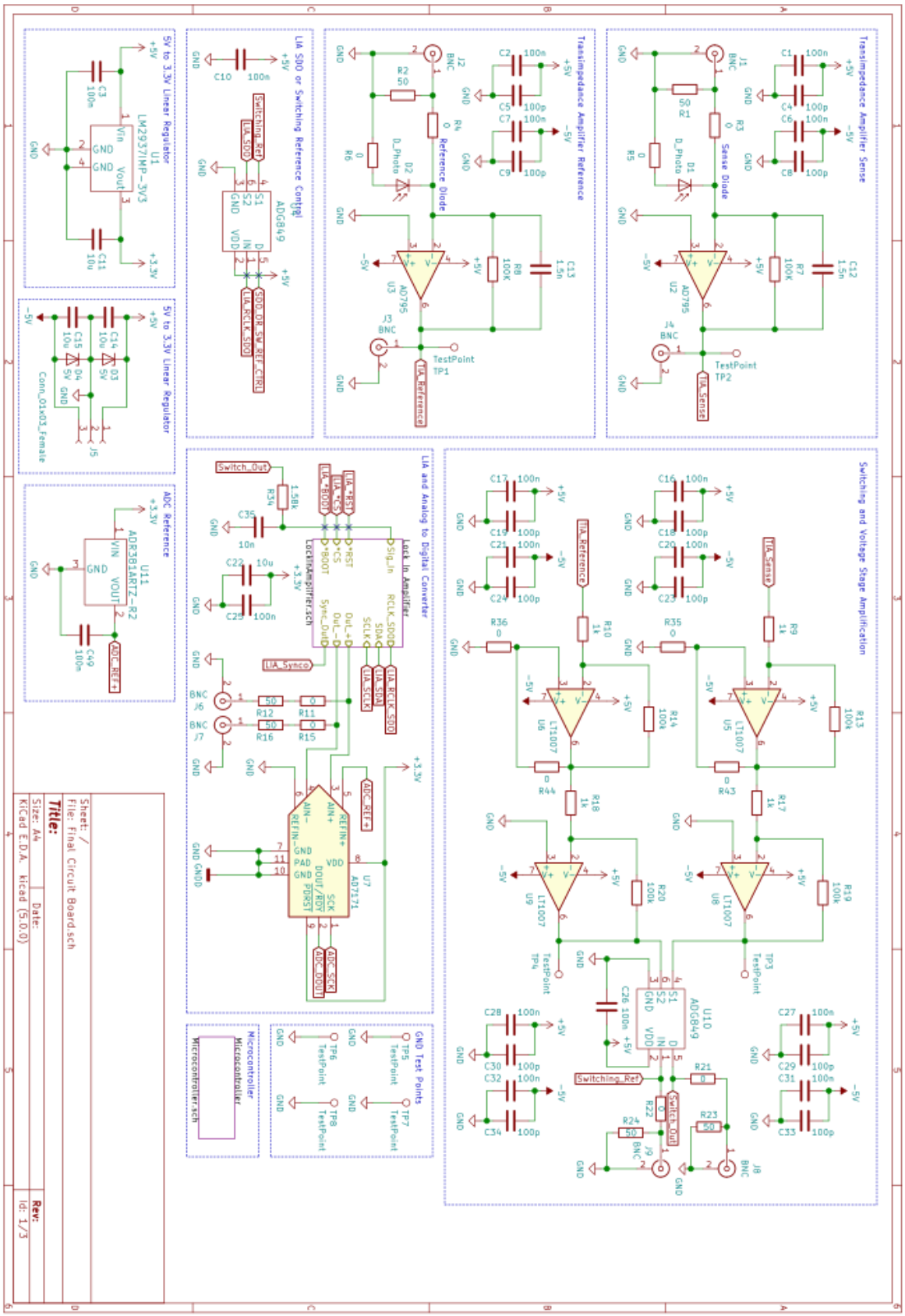

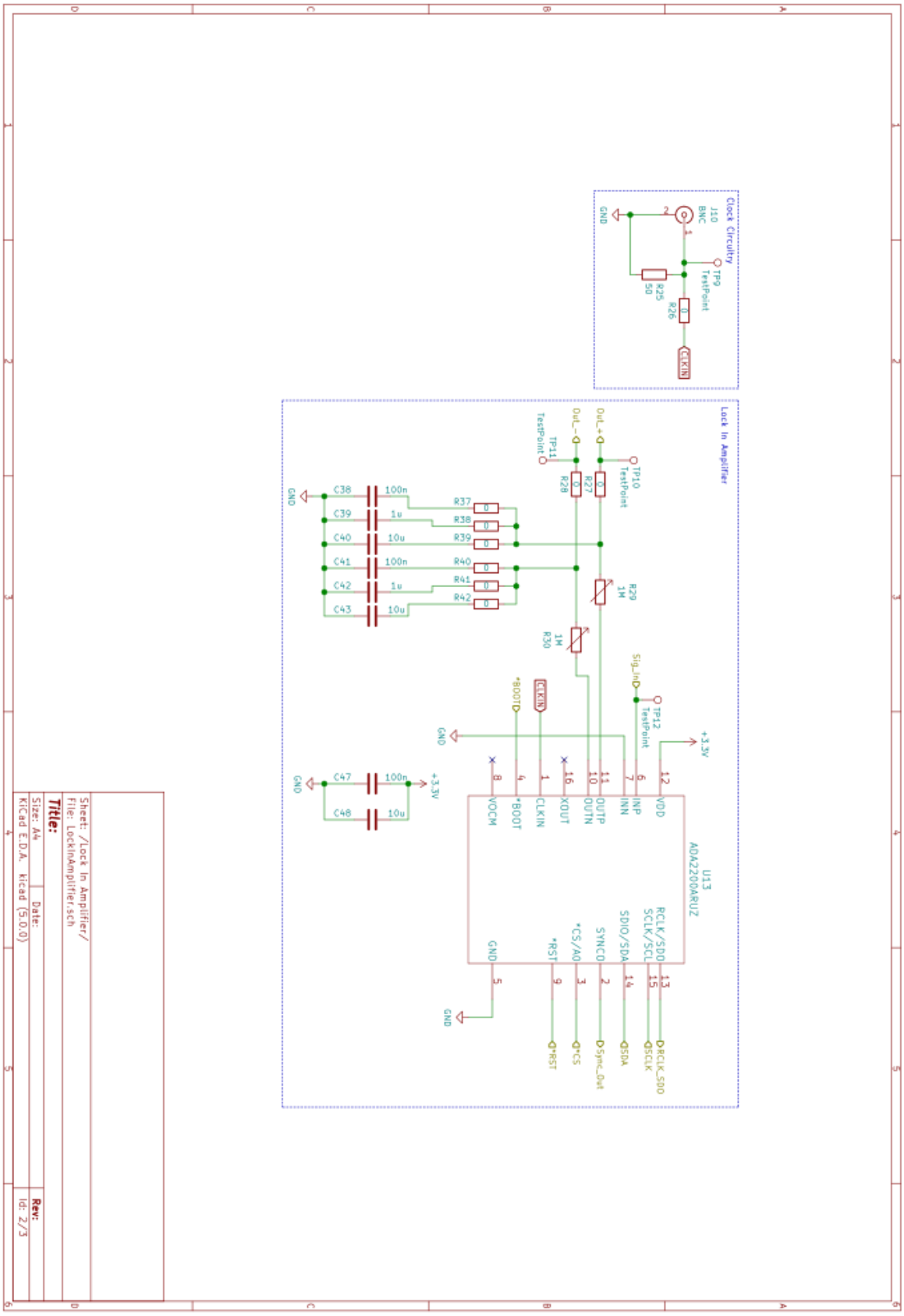
Clock Circuitry
Lock In Amplifier
Sheet: /Lock In Amplifier/
File: LockInAmplifier.sch
Title:
Size: A4
Date:
Rev:
KiCad E.D.A. kicad (5.0.0)
Id: 2/3

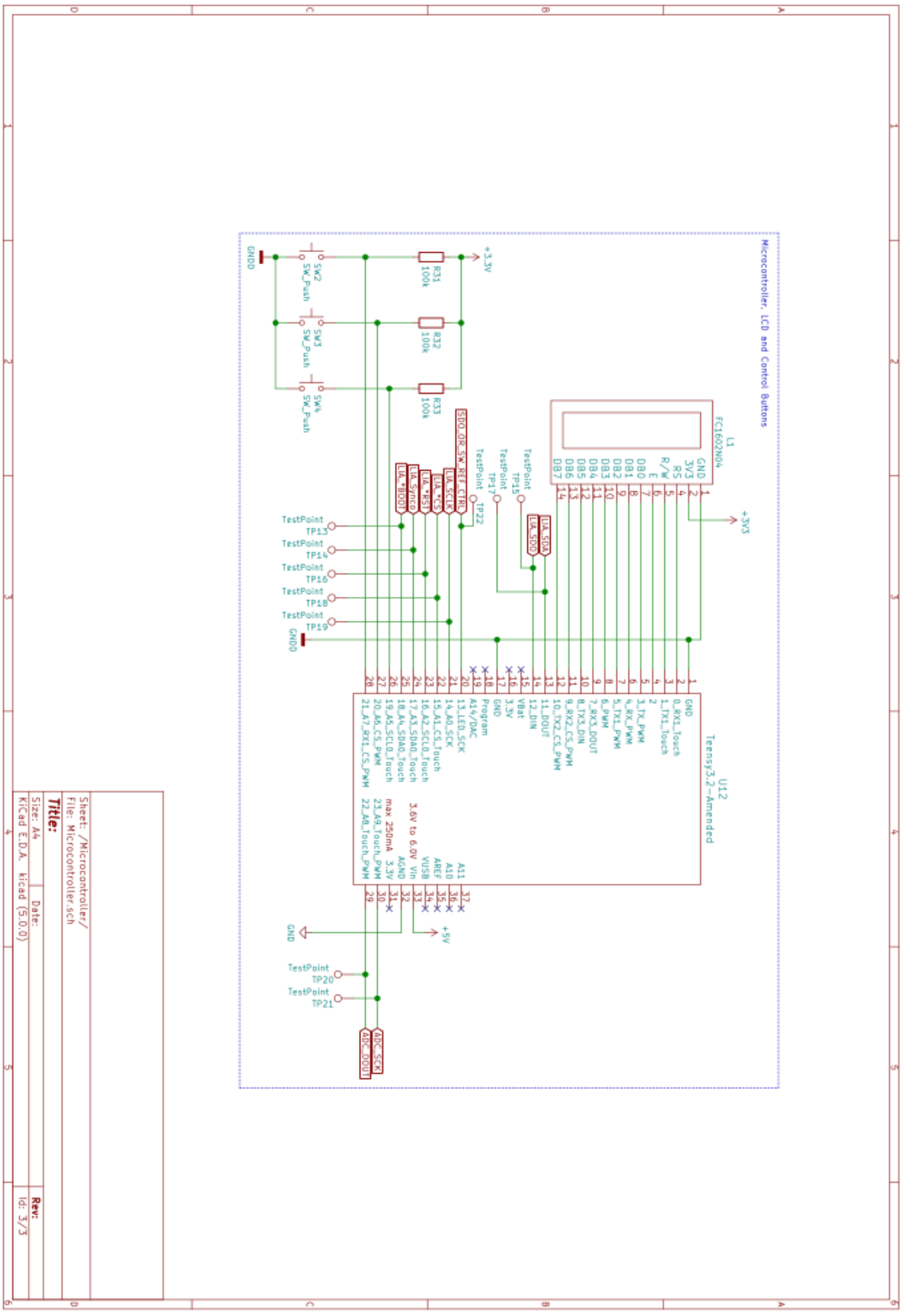
Microcontroller, LCD and Control Buttons
Teensy3.2-Amended
U12
FC1602N04
L1
SW2
SW_Push
SW3
SW4
R31
R32
R33
100k
+3.3V
+3V3
+5V
GND
TestPoint
TP13
TP14
TP16
TP18
TP19
TP15
TP17
TP22
TP20
TP21
LIA_SDA
LIA_SCL
LIA_SYNCO
LIA_*RST
LIA_*CS
LIA_*BUSY
SDO_OR_SW_REF_CTRL
ADC_SCLK
ADC_DOUT
3.6V to 6.0V
max 250mA
Sheet: /Microcontroller/
File: Microcontroller.sch
Title:
Size: A4
Date:
KiCad E.D.A. kicad (5.0.0)
Rev:
Id: 3/3

Appendix D – Completed PCB Design 3D Renders

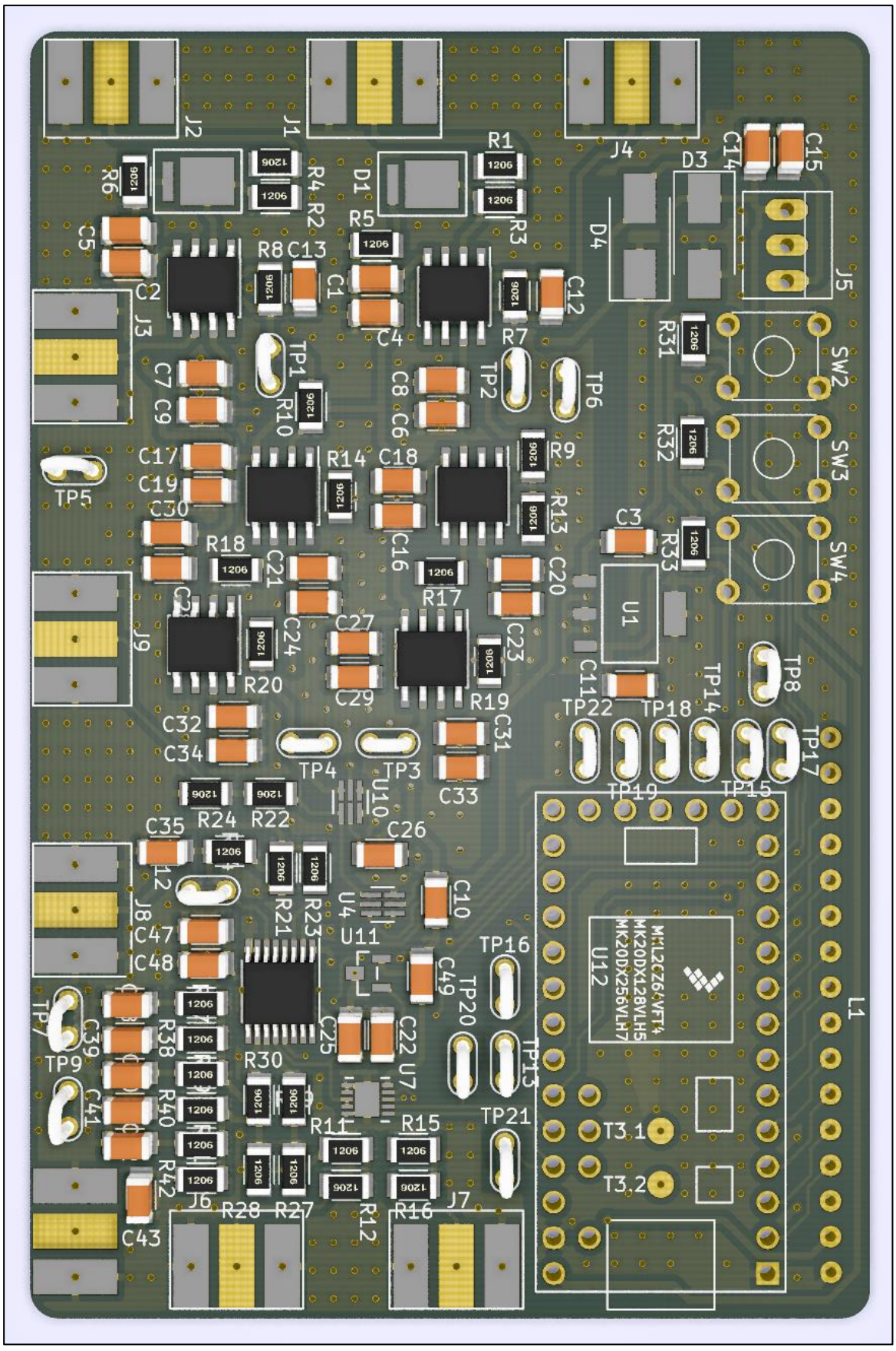

Appendix E – Black Body Source Testing Setup

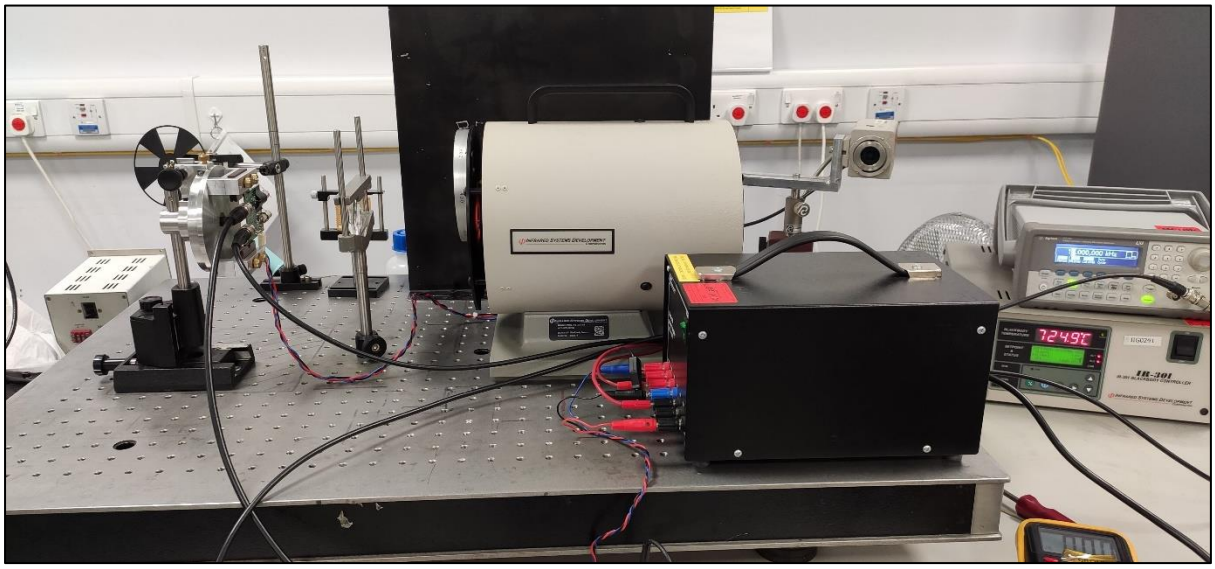

Appendix F – TIA Testing Circuit Board

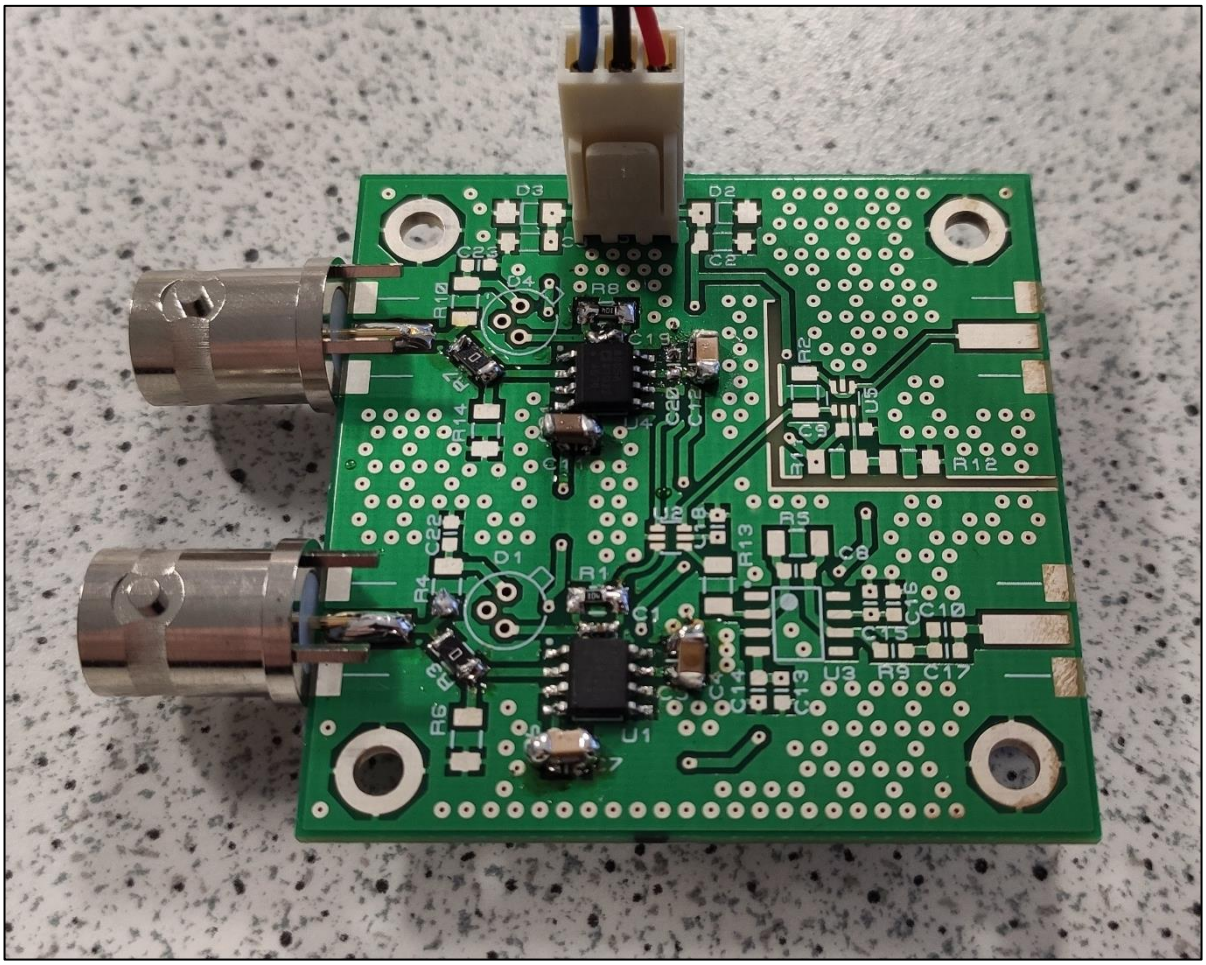

Appendix G – Project Schedule

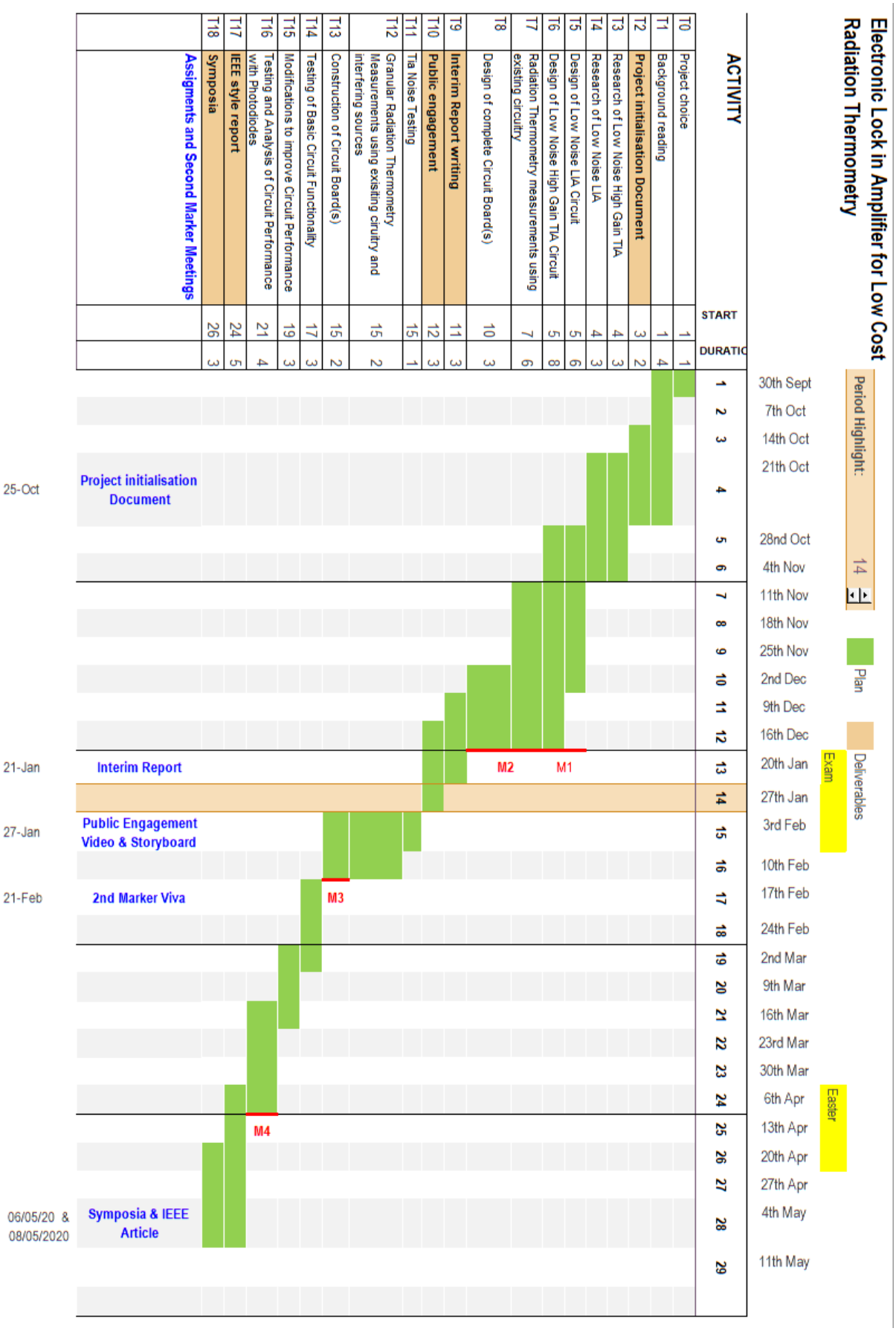

Appendix H – Risk Register

Risk Number	Description of Risk	Existing Control Measures	Risk Likelihood (1 - 5)	Risk Severity (1 - 5)	Risk Score (0 - 25)	Additional Control Measures	Amended Risk Likelihood (1 - 5)	Amended Risk Severity (1 - 5)	Amended Risk Score (0 - 25)
1	Loss of Project Data	Project data is stored on a Desktop and Laptop computer. Additionally, it is periodically backed up on Google Drive. Development files (Schematics, PCB Layouts, etc.) will be stored in a Git repository with full history and version control.	1	5	5	**No additional measures required.**	N/A	N/A	N/A
2	Exceeding Project Budget	The EEE department controls all purchasing for 3rd year projects. Components can only be purchased through approved suppliers by EEE staff. Thus, overbudget projects are prohibited. A full costing breakdown will be compiled in a spreadsheet for the project.	1	4	4	**No additional measures required.**	N/A	N/A	N/A
3	Missing Deliverable Deadlines	A Gantt Chart has been created to outline a schedule for project progress against individual specification points. The Gantt Chart will be reviewed on a fortnightly basis (at minimum) with the project supervisor to ensure key project deadlines are met.	1	4	4	**No additional measures required.**	N/A	N/A	N/A
4	Working Time lost due to Injury	Before any practical work is completed a full risk assessment must be completed and signed by the project supervisor. This risk assessment should identify and mitigate any foreseeable project risk.	1	4	4	**No additional measures required.**	N/A	N/A	N/A
5	Incorrect PCB Design	PCB Design package used to simplify the design process and lower the likelihood of mistakes. A full simulation of the circuit in SPICE should be completed before committing to hardware design. A design review will be completed before ordering the finished PCB design. PCB(s) should be ordered before the winter holiday (2019/20) to allow for testing and redesign in the Spring Semester.	2	4	8	The PCB should be designed accounting for modification during the testing phase. This allows for changes without a full PCB redesign. **Risk expires once testing phase has been completed.**	2	2	4
6	Failure of Black Body Test Equipment	Equipment is maintained and managed by staff running the EEE B12 Laboratory.	1	4	4	**No additional measures required. Risk expires when Black Body testing is complete.**	N/A	N/A	N/A
7	No access to George Porter F13 Lab due to delayed movement to Mappin Building	Movement from Mappin Building planned for January, outside of term time. Diamond E&C Laboratory and iForge available as a back up space for working.	3	3	9	Induction to B12 Laboratory completed. B12 can be used as an additional back up Laboratory.	3	1	3
8	Construction of High Gain (approximately 10 Million to 1 Billion) Low Noise TIA too complex/not possible	Research of a wide range of low noise TIA construction methodologies. Early research of available Operational Amplifier GBW values to evaluate the possibility of a 1 Billion gain value.	3	4	12	Perform additional research of alternative methods for producing a Photodiode front end that can measure pA signals.	3	2	6
9	Required components for pA capable TIA/LIA circuit are too expensive for project budget	Research TIA/LIA designs that provide the minimum required functionality based upon the specification. Limit PCB design to two layers. Individual Project budgets have been extended to £200 this year.	3	4	12	Perform additional research of alternative methods for producing a Photodiode front end that can measure pA signals.	3	2	6
10	Component obsolescence during development	Use the newest version of a component that exists, where reasonably practicable. Attempt to use components that have been released fairly recently. Periodically check for component obsolescence. Order replacement components.	2	4	8	**No additional measures required. Risk expires when PCB is fully tested.**	N/A	N/A	N/A

Risk Severity	Risk Likelihood				
	1	2	3	4	5
1	1	2	3	4	5
2	2	4	6	8	10
3	3	6	9	12	15
4	4	8	12	16	20
5	5	10	15	20	25

Appendix I – Purchase Order Form

Item Name	Supplier	Supplier Stock Number	Item Cost	Item Quantity	Total Cost
1.5n	Farnell	1759339RL	£0.09	10	£0.90
10u	Farnell	3013526	£0.20	10	£2.03
1u	Farnell	9227865	£0.12	10	£1.22
5V Zener Diode	Farnell	1431161	£0.34	10	£3.44
FC1602N04 LCD	Farnell	2674133	£12.14	1	£12.14
50	Farnell	2057745	£0.05	10	£0.46
100K	Farnell	9241060	£0.06	10	£0.58
1k	Farnell	1469965	£0.08	10	£0.75
1M	Farnell	1469968	£0.08	10	£0.75
1.58k	Farnell	2307421	£0.06	10	£0.56
Tactile Switch 6x6mm	Farnell	1608274	£0.22	5	£1.08
LM2937IMP-3V3	Farnell	3122675	£1.64	2	£3.28
AD795	Farnell	1651296	£7.90	4	£31.60
ADG849	Farnell	1651265	£1.70	4	£6.80
LT1007	RS Components	761-7911	£4.10	8	£32.80
AD7171	Farnell	1827293	£2.84	3	£8.52
ADR381ARTZ-R2	Farnell	1651177	£1.00	3	£3.00
			Grand Total		£109.92

Personal Development Plan

This section briefly covers my plans for personal development over the coming six months, as well as reflecting upon the previous term of the course.

What modules do you like?

Of all modules this year, the individual construction project (EEE381) is my personal favourite. I enjoy the freedom I have to design circuits, tests and experiments to obtain the information and results I need. I look forward to continuing work on this project over the coming term. EEE348 and EEE339 have also been engaging, in particular the content covered by Dr Maiden and the Microprocessor Architecture section covered by Mr Powell.

What modules don't you like?

At present, the Finance and Law module (MGT388) is my least favourite of the year. The law component of the module is clearly and concisely taught, with a depth that seems relevant to our course. However, the Finance content seems overly complicated for engineers, with too much focus on specific terminology and calculations. More focus on the decision making process would be useful.

What is not going well?

At present I wouldn't say anything about the course is not going well. With the extracurricular projects I am involved in time management is a key skill, especially in 3rd year. However, at present I believe everything is in a manageable state.

What are you struggling with?

Writing concise reports is a difficulty for me at present. Understanding what sections of work are most relevant for a report and which can be left out is a difficult task. This has been compounded during the 3rd Year Project due to the amount of work conducted over the time period. As it is a longer project, there is much more to talk about.

What are your goals for the next six months?

My goals for the next six months to a year are as follows:

- Start a further Summer Placement with Siemens Congleton.
- Organise a fourth year university project in collaboration with Siemens, working on a real industrial problem.
- Produce a successful report and presentation for Tinsley Bridge surrounding Data Driven Manufacturing applications for their site as part of the 2nd year SELA project.
- Produce a successful Electronic Lock-in Amplifier design!
- Produce a successful control interface for the Avalon ROV project. In particular using Test Driven Development and maintainable code practices for the robot serial interface.
- Attempt to gain guidance and feedback on report writing, in preparation for future 3rd year project reports.